JVI Accepted Manuscript Posted Online 4 February 2015
J. Virol. doi:10.1128/JVI.03274-14

ATP1A1-mediated Src signaling inhibits coronavirus entry into host cells

Christine Burkard[a✦], Monique H Verheije[a*], Bart L Haagmans[b], Frank J van Kuppeveld[a], Peter J M Rottier[a], Berend-Jan Bosch[a], Cornelis A M de Haan[a#]

Virology Division, Department of Infectious Diseases and Immunology, Faculty of Veterinary Medicine, Utrecht University, Utrecht, The Netherlands[a]; Department of Viroscience, Erasmus MC, Rotterdam, The Netherlands[b]

Running Head: Na^+,K^+-ATPase signaling prevents viral entry

Address correspondence to Cornelis A M de Haan, c.a.m.dehaan@uu.nl

✦ Present address: The Roslin Institute and Royal (Dick) School of Veterinary Studies, University of Edinburgh, Easter Bush, Edinburgh EH25 9RG, UK

* Present address: Department of Pathobiology, Division Pathology, Faculty of Veterinary Medicine, Utrecht University, Utrecht, The Netherlands

Abstract

Besides by transporting ions the multi-subunit Na^+,K^+-ATPase also functions by relaying cardiotonic steroid-binding induced signals into cells. In this study we analyzed the role of Na^+,K^+-ATPase and in particular of its ATP1A1 α-subunit during coronavirus (CoV) infection. As controls, the vesicular stomatitis virus (VSV) and influenza A virus (IAV) were taken along. Using gene silencing, the ATP1A1 protein was shown to be critical for infection of cells with murine hepatitis virus (MHV), feline infectious peritonitis virus (FIPV) and VSV, but not with IAV. Lack of ATP1A1 did not affect virus binding to host cells, but resulted inhibited entry of MHV and VSV. Consistently, nanomolar concentrations of the cardiotonic steroids ouabain or bufalin, which are known not to affect the transport function of Na^+,K^+-ATPase, inhibited infection of cells with MHV, FIPV, MERS-CoV, and VSV, but not IAV, when the compounds were present during virus inoculation. Cardiotonic steroids were shown to inhibit entry of MHV at an early stage, resulting in accumulation of virions close to the cell surface and as a consequence in reduced fusion. In agreement with an early block in infection, the inhibition of VSV by CTSs could be bypassed by low-pH shock. Viral RNA replication was not affected when these compounds were added after virus entry. The anti-viral effect of ouabain could be relieved by the addition of different Src kinase inhibitors, indicating that Src signaling mediated via ATP1A1 plays a crucial role in the inhibition of CoV and VSV infections.

Importance

Coronaviruses (CoVs) are important pathogens of animals and humans as demonstrated by the recent emergence of new human CoVs of zoonotic origin. Antiviral drugs targeting CoV infections are lacking. In the present study we show that the ATP1A1 subunit of Na^+,K^+-ATPase, an ion

43 transporter and signaling transducer, supports CoV infection. Targeting ATP1A1 either by gene
44 silencing or by low concentrations of the ATP1A1-binding cardiotonic steroids ouabain and
45 bufalin, resulted in inhibition of infection with murine, feline and MERS-CoVs at an early entry
46 stage. Infection with the control virus VSV was also inhibited. Src signaling mediated by ATP1A1
47 was shown to play a crucial role in the inhibition of virus entry by ouabain and bufalin. These
48 results suggest that targeting the Na^+,K^+-ATPase using cardiotonic steroids, several of which are
49 FDA-approved compounds, may be an attractive therapeutic approach against CoV and VSV
50 infections.
51
52

Introduction

Despite the wide variety of vaccines already available to prevent viral infections, unexpected epidemics caused by zoonotic viruses, such as SARS-CoV in 2002/03 and the new pandemic H1N1 influenza A virus (IAV) in 2009, underscore the need for additional antiviral measures. Compound- and siRNA screening may aid the development of antiviral therapies by the discovery of lead compounds and target proteins (1-3). Elucidating the mechanisms by which such proteins act during infection and how drugs can interfere with the pathogen life cycle is of crucial importance herein.

Coronaviruses (CoVs) are enveloped, plus-strand RNA viruses of the *Coronaviridae* family in the order *Nidovirales.* These viruses generally cause respiratory and/or intestinal tract disease. CoVs are important pathogens of domestic livestock, poultry and companion animals as exemplified by porcine epidemic diarrhea virus, infectious bronchitis virus, and feline infectious peritonitis virus (FIPV), respectively. In addition, the emergence of new human CoVs of zoonotic origin has shown the potential of CoVs to cause life-threatening disease in humans as was demonstrated by the 2002/2003 SARS-CoV epidemic and by the recent emergence of MERS-CoV (4, 5). The murine hepatitis coronavirus (MHV) is often employed as a safe model to study CoV infections.

Like all other viruses, CoVs depend on the cellular machinery for efficient infection and replication in their host cells. The CoV infection cycle starts with attachment of the virus to a specific cellular receptor, mediated by the viral spike protein (S). Upon endocytic uptake, which has been demonstrated to occur via clathrin-mediated endocytosis for MHV (6), conformational changes in the S protein induce virus-cell fusion. The genomic RNA is thereby released into the

cytoplasm and becomes translated, resulting in the formation of RNA replication-transcription complexes associated with rearranged cellular membranes (7). Structural proteins together with newly generated genomic RNAs assemble into progeny virions via budding through the membranes of the ER-to-Golgi intermediate compartment. Virions are subsequently released via exocytosis (8).

The Na^+,K^+-ATPase is perhaps one of the best studied membrane ion transporters. Discovered in 1957 and identified as an ion-activated ATPase in 1965, it is mainly known for its transport function of K^+ and Na^+ at a ratio of 2:3, creating an electrochemical gradient across the plasma membrane (9). The Na^+,K^+-ATPase consists of two functional (α and β) and one regulatory subunit (γ subunit or FXYD protein). The α-subunit is a large, catalytical membrane protein, containing 10 transmembrane domains that create five extracellular and four intracellular loops. Four different isoforms of the α-subunit exist, which are encoded by *ATP1A1-4*. The α1-isoform is ubiquitously expressed in almost all tissues. The β-subunit is a type II membrane protein, responsible for the proper translocation of the α-subunit into the endoplasmic reticulum and its delivery to the cell surface and is crucial to the functioning of the pump. Little is known about the function of the regulatory subunit γ (reviewed in (10)). Specific inhibitors of the Na^+,K^+-ATPase, so called cardiotonic steroids (CTSs), can block the transport function of the pump and are used to treat congestive heart failure. Well-known CTSs are the foxglove plant-derived digoxin and ouabain, and the vertebrate-derived analogues bufalin and marinobufagenin (11, 12).

In addition to the classical ion-pumping function of the Na^+,K^+-ATPase, more recent work has shown additional roles of Na^+,K^+-ATPase in signal transduction. Especially the α-subunit appears to be associated with a number of additional proteins and to carry out various signaling functions

(reviewed in (13, 14)), which may differ between the different α-subunit isoforms (15). (Endogenous) CTSs can trigger the signaling functions of the Na^+,K^+-ATPase at concentrations that do not affect the pump function or intracellular ion concentration (16-21). There are four main signaling targets of α-subunit known so far; PI3K, Src, IP3R, and PLC. Binding of nanomolar concentrations of ouabain to Na^+,K^+-ATPase triggers a conformational change in the α-subunit, which activates the bound Src protein and results in the recruitment of other signaling factors. Binding of ouabain to Na^+,K^+-ATPase activates tyrosine phosphorylation of Src and of other proteins. Activation of these targets may lead to a number of downstream signaling effects controlling apoptosis, cell-cell interaction, gene-expression, as well as other processes (16-18, 22-28).

In a high-throughput RNAi screen we previously identified ATP1A1 as a protein that supports MHV infection (unpublished results). ATP1A1 is an appealing antiviral target in view of the large number of (FDA-approved) compounds available that target this protein. Therefore, the main goal of the present study was to obtain mechanistic insight into the role of the Na^+,K^+-ATPase in CoV infection. Targeting ATP1A1 either by gene silencing or by low concentrations of CTSs ouabain and bufalin resulted in inhibition of CoV infection at an early entry stage. As controls the well-studied vesicular stomatitis virus (VSV) and influenza A virus (IAV) were taken along. Src signaling mediated by ATP1A1 was shown to play a crucial role in the inhibition of CoV and VSV entry by CTSs. These results suggest that targeting the Na^+,K^+-ATPase using CTSs may be an attractive therapeutic approach against CoV and VSV infections.

Materials and Methods

Cells, viruses, and plasmids.

Murine LR7 (29) (murine L-2 fibroblast cells (ATCC), stably expressing murine CEACAM1a (mCC1a), and feline FCWF cells (ATCC) were used to propagate the (recombinant) MHV and FIPV viruses, respectively. HEK293T, MDCK-HA and Huh7 cells were used to propagate pseudotyped VSVΔG/Luc-G*, *Renilla* luciferase expressing IAV-WSN pseudovirus (IAV-Rluc) or MERS-CoV, respectively, as described previously (30-32). Cells were maintained as monolayers cultured in Dulbecco's modified Eagle's medium (DMEM, Lonza), supplemented with 10% fetal bovine serum (FBS). HeLa-ATCC cells stably expressing mCC1a (HeLa-mCC1a;(6)) HeLa-fAPN cells (33), and HeLa-ATCC were used for infection experiments with MHV, FIPV, and VSV, respectively. HeLa-ATCC and HeLa-mCC1a cells stably expressing the defective β-galactosidase ΔM15 (HeLa-(mCC1a-)ΔM15) were used in entry assays (34). Generation of recombinant viruses MHV-EFLM (35), FIPV-Δ3abcRL (36), IAV-Rluc pseudovirus (30), MHV-αN (34), VSVΔG/Luc-Gα* (34), MHV-2aFLSRec (37), and MHV-S2'FCS (6) has been described previously. MHV-2aGFPSRec, which contains a GFP expression cassette between the 2a and the S gene at the position of the HE pseudogene was generated similarly as described for MHV-2aFLSRec (37). cDNAs encoding human or mouse ATP1A1 were obtained from Thermo Scientific Open biosystems. ATP1A1 cDNAs were subcloned into a pCAGGS expression vector, using conventional cloning methods, thereby generating pCAGGS-hATP1A1 and pCAGGS-mATP1A1.

Chemicals.

The MHV fusion inhibitor HR2 peptide has been described before (38) and was synthesized by GenScript. The peptide was diluted in Tris/HCl 50 mM, pH7.8, 4 μM EGTA at 1 mM stock solution

and used at 10 μM final concentration. Stocks of 125 μM bafilomycin A1 (BafA1, Enzo Life Sciences), 15 mM Dyngo-4a (Dyngo, Abcam), 500 μM wortmannin (Wort, Enzo Life Sciences), 10 mM PP2 (Sigma), and 10 μM bufalin (Buf, Enzo Life Sciences) were prepared in DMSO and diluted 1:1000 in the experiments, except when indicated otherwise. Stocks of 10 mM chlorpromazine (Chlopro, Sigma), 20 mM U18666A (Enzo Life Sciences), 50 μM ouabain (Ou, Sigma) were prepared in H_2O and diluted 1:1000 in the experiments, except when indicated otherwise. pNaKtide peptide (39), which was kindly provided Z. Xie (Marshall University, Institute for Interdisciplinary Research), was dissolved in PBS at 2 mM and used at 2 μM final concentration. Solvent DMSO was obtained from Sigma-Aldrich.

siRNA transfections.

In assays using luciferase-based read-outs 96-well plates were used. For other assays a 24-well plate format was used. 7,500 or 30,000 HeLa-mCC1a or HeLa-fAPN cells were seeded one day prior to transfection in each well of the 96-well or 24-well plate, respectively. Using Oligofectamine (Life Technologies) reagent three independent, non-overlapping siRNAs (Ambion) targeting ATP1A1 were individually transfected into target cells according to the manufacturer's instructions. Transfection mix for four wells (96-well format) or 1 well (24-well format) contained 2.5 μl of 1 μM siRNA and 0.5 μl Oligofectamine in 50 μl OptiMEM (Gibco). Transfection was done in 62.5 μl or 250 μl final volume of OptiMEM, while 4 hours post transfection 32 μl or 125 μl of DMEM, 30% FBS were added, depending on the plate format used. Cells were infected 72 hours post transfection.

qRT-PCR of siRNA-mediated gene knockdowns.

HeLa-mCC1a cells were subjected to siRNA-mediated gene knockdown as described above. At 72 hpi cells were harvested by trypsinization, single-cell suspension counted, and collected by centrifugation. Cellular RNA was extracted using the RNeasy Mini Kit (Qiagen). mRNA levels of genes were analyzed by qRT-PCR using a custom designed pair of specific primers to the gene resulting in an approximately 150 bp product. RNA levels were measured using the GoTaq® 1-Step RT-qPCR system (Promega) according to the manufacturer's instructions on a LightCycler 480 (Roche). Expression levels were corrected for cell number and viability as determined by the Wst-1 assay (Roche), which were hardly affected, if at all, however by transfection of the siRNAs.

Virus infections.

Cells were inoculated with MHV-EFLM, FIPV-RLuc, IAV-RLuc, VSVΔG/Luc-G*, MHV-S2'FCS, or MHV-2aFLSRec at MOI=0.1 in DMEM, 2% FBS, for 2 h at 37°C. Cells were lysed at 7 hpi (MHV, FIPV, and VSV) or 16 hpi (IAV) in passive lysis buffer (Promega). Firefly luciferase expression was assessed using the firefly luciferase assay system from Promega or using a homemade system (50 mM tricine, 100 μM EDTA, 2.5 mM $MgSO_4$, 10 mM DTT, 1.25 mM ATP, 12.5 μ D-Luciferin). *Renilla* luciferase expression was assessed using the *Renilla* luciferase assay system (Promega). Light emission was measured on a Centro LB 960 luminometer. When indicated cells were transfected with siRNAs prior to inoculation as described above. Luciferase expression levels (in relative light units, RLU) were corrected for cell number and viability as determined by the Wst-1 assay (Roche). When indicated cells were treated with pharmacological inhibitors starting at 30 min prior to or 2 h post inoculation.

At 72 h after transfection, siRNA transfected cells were inoculated with MHV-2aGFPSRec at MOI=0.5 (15-20% infected cells) in DMEM, 2% FBS, for 2 h at 37°C. The inoculum was replaced

193 by warm DMEM, 10% FBS. At 8 hpi, cells were trypsinized and fixed in 4% formaldehyde solution
194 in PBS. Cells were washed and taken up in FACS buffer (2% FBS, 0.05M EDTA, 0.2% NaN_3 in PBS)
195 and GFP expression was quantified by FACS analysis on a FACS Calibur (Benson Dickson) using
196 FlowJo software. Of each sample at least 10,000 cells were analyzed.
197
198 Vero cells were inoculated with MERS-CoV at a MOI of 0.1 in FBS-containing DMEM. 8 h post
199 infection, cells were fixed in 4% formaldehyde in PBS. Cells were stained using rabbit anti-SARS-
200 CoV nsp4 antibodies that are cross-reactive for MERS-CoV, according to a standard protocol
201 using a FITC-conjugated swine-anti-rabbit antibody. Number of infected cells was determined by
202 cell counts on a wide-field fluorescent microscope. Cells were treated with ouabain or bufalin
203 starting at 30 min prior to or 2 h post inoculation.
204
205 **Binding, internalization and fusion assays using β-galactosidase complementation.**
206 The replication-independent binding, internalization, and fusion assays were performed as
207 described previously (34). The assay is based on complementation of an otherwise defective β-
208 galactosidase ΔM15 protein by a small intravirion peptide that is genetically fused to the N
209 protein. Briefly, in the binding and internalization assay MHV-αN or VSVΔG/Luc-Gα* virus was
210 bound to HeLa-(mCC1a-)ΔM15 target cells at MOI=10 for 90 min on ice. In the binding assay
211 unbound virus was removed and cells and viruses lysed with NP-40 lysis buffer buffer (50 mM
212 Tris/HCl pH 8.0, 150 mM NaCl, 0.5% NP-40). Complementation was analyzed using a Centro LB
213 960 luminometer (Berthold technologies). 30µl/well Beta-Glo reagent (Promega) was added to
214 each well, the sample was mixed and incubated for 60 min and light units were measured over
215 0.1 second. In the internalization assay unbound virus was removed after binding and cells
216 shifted to 37°C for 30 or 60 min, for VSV and MHV, respectively. Cells were trypsinized to remove

surface-bound but not internalized virus. Cells were lysed and complementation measured as described above. Dependent on the experiment type cells were transfected with siRNA for 72h as described above or pre-treated with drugs for 30 min prior to binding or internalization experiments.

To assay fusion cells were preloaded with FDG substrate by incubation of adherent target cells with 2.5% FBS, 100 mM FDG, 50% PBS at room temperature. After 3 min incubation an excess of 5% FBS in PBS was added, supernatant removed and replaced by growth medium. When pharmacological inhibitors were used cells were (mock) treated with the different inhibitors for 30 min after a recovery period of 30 min at 37°C. MHV-αN or VSVΔG/Luc-Gα* virus was bound to cells in DMEM with 2%FCS (in the absence or presence of inhibitors) at a MOI=20 for 90 min at 4°C to synchronize infection, after which cells were shifted to 37°C for 2 h. Cells were trypsinized and transferred to Eppendorf tubes, washed and immediately analyzed by FACS. siRNA transfections were performed 72h prior to fusion assays.

Ouabain time of addition experiment

MHV-EFLM virus was bound to HeLa-mCC1a cells on ice at MOI=0.5 for 90 min. Warm medium containing 10% FBS was added and cells incubated for 7h at 37°C, 5% CO_2. At time points indicated the medium was replaced by warm medium containing 50nM ouabain. 7 hpi cells were lysed and luciferase expression analyzed as described above.

Effect of ouabain on virus entry using fluorescently labeled MHV.

DyLight 488 covalently labeled MHV virus was made as described before (6). Briefly, MHV strain A59 virus was grown in LR7 cells and purified using a sucrose cushion and gradient purification.

After purification virus was labeled using DyLight NHS 488 (Thermo Scientific) according to the manufacturer's instructions. Infectivity of the labeled virus was confirmed by TCID50 analysis and qRT-PCR. Fluorescently labeled virus was bound to cells, either mock treated or pre-treated with ouabain for 30 min, on ice at MOI=10 for 90 min. Unbound virus was removed and virus allowed to infect for 90 min in presence or absence of ouabain. Cells were subsequently fixed and stained with DAPI (Invitrogen) and Alexa Fluor 568 Phalloidin (Life Technologies). The samples were analyzed using a confocal laser-scanning microscope (Leica SPE-II).

Low pH bypass of endocytic uptake by VSV via direct fusion at the plasma membrane

HeLa-ATCC cells were pre-treated with medium containing 50nM ouabain for 30min at 37°C. Following pre-treatment, VSVΔG/Luc-G* was bound to cells at MOI=0.3 in presence of 50nM ouabain at 4°C. Inoculum was removed and unbound virus washed away with ice-cold PBS. Cells were incubated for 2h at 37°C in presence of ouabain. At 2hpi supernatant was removed and warm buffers at different pH (7.2, 6.5, 5.5, and 5.0) containing 50nM ouabain were added for 2 min. Buffers were removed and cells incubated at 37°C in medium containing 50nM ouabain. Infection levels were determined by measuring the luciferase expression levels in the cell lysate at 9hpi.

Results

RNAi-mediated gene silencing of ATP1A1 inhibits infection with MHV and FIPV but not IAV.

In a high-throughput RNAi screen ATP1A1 was found to be required for efficient infection of HeLa cells with MHV. To validate this finding and to see whether ATP1A1 is also required for infection with other CoVs, we performed a follow-up analysis using siRNA-mediated gene silencing with oligonucleotides from a different supplier. HeLa cells or HeLa cells carrying the receptor for MHV (HeLa-mCC1a cells) or for FIPV (HeLa-fAPN) were transfected with siRNAs for 72h. Subsequently, cells were infected with luciferase expressing MHV (MHV-EFLM, (35)), FIPV (FIPV-Δ3abcRL; (36)), IAV (IAV-RLuc; (30)), or VSV (VSVΔG/Luc-G*; (32)) at a multiplicity of infection (MOI) of 0.1. At 7 hpi (MHV, FIPV, and VSV) or 16 hpi (IAV), cells were lysed and luciferase expression levels were determined. As negative controls, scrambled siRNAs were used. Individual transfection of each of the three siRNAs targeting ATP1A1 resulted in reduced infection of cells with MHV, FIPV, and VSV. IAV infection was not affected by siRNA-mediated gene silencing of ATP1A1 (fig. 1A). To confirm the efficacies of the siRNAs at the mRNA level, quantitative RT-PCR analysis was performed. All three siRNAs reduced the ATP1A1 mRNA levels with approximately 95% (fig. 1B). From these results we conclude that ATP1A1 is required for efficient infection of cells with MHV, FIPV, and VSV, but not IAV.

RNAi-mediated gene silencing of ATP1A1 inhibits fusion signal of MHV and VSV.

To investigate whether the siRNA-mediated silencing of ATP1A1 affected entry of MHV we made use of a recently developed, replication-independent binding, internalization, and fusion assay (34). The assay is based on minimal complementation of defective β-galactosidase (β-

283 galactosidase ΔM15) with the short α-peptide (40) that is genetically fused to the intravirion N
284 protein in MHV-αN. Prior to virus binding, ΔM15-expressing cells were transfected with siRNAs
285 for 72h. After binding of virus particles to cells on ice unbound viruses were removed and cells
286 and viruses were lysed (binding assay). In the internalization assay MHV-αN was bound to cells
287 on ice, unbound virus was removed, and virus was subsequently allowed to internalize at 37°C
288 for 60 min, after which cell-surface bound virus particles were removed by protease treatment
289 prior to lysis of cells and viruses. Virus particle binding and internalization into cells were
290 quantified by measuring the amount of luminescence generated after addition of Beta-Glo
291 substrate to the cell lysate. As shown in Figure 2, both virus binding and internalization did not
292 appear to be affected by siRNA-mediated silencing of ATP1A1. To measure fusion, MHV-αN was
293 bound to cells pre-loaded with fluorescein-di-β-D-galactopyranoside (FDG). After binding virus
294 was allowed to internalize and fuse. Conversion of the non-fluorescent substrate FDG by
295 reconstituted β-galactosidase into the green fluorophore fluorescein (FIC) in intact cells was
296 measured by FACS. Please note that viral fusion signals can also be inhibited by interference with
297 essential processes that precede viral fusion. In contrast to virus binding and internalization,
298 fusion of MHV was inhibited by the lack of ATP1A1 relative to the negative-control siRNAs (fig.
299 2A). siRNA-mediated gene silencing of ATP1A1 also inhibited the fusion signal of VSV as
300 determined with a VSV fusion assay (34) that just as for MHV is based on minimal
301 complementation of defective β-galactosidase (fig. 2B).
302
303 **RNAi-mediated gene silencing of ATP1A1 inhibits infection with MHV independent of the**
304 **intracellular site of fusion or the identity of the receptor.**
305 Trafficking of MHV and FIPV to lysosomes is a prerequisite for proteolytic activation of the S
306 protein and for efficient virus-cell fusion to occur (6). To study whether downregulation of

ATP1A1 inhibits MHV infection by negatively affecting the trafficking of MHV to lysosomes, we made use of a mutant MHV (MHV-S2'FCS), which is cleavage-activated by furin rather than lysosomal proteases, and which hence fuses in early endosomes (6). Thus, HeLa-mCC1a cells were transfected with siRNAs for 72h, followed by inoculation with luciferase expressing MHV (MHV-EFLM) or MHV-S2'FCS at MOI=0.1. At 7 hpi cells were lysed and firefly luciferase expression levels were determined. As shown in figure 3A, transfection of siRNAs targeting ATP1A1 reduced luciferase expression levels to the same extent for both viruses. From these results we conclude that infection with MHV is negatively affected by downregulation of ATP1A1 regardless of the intracellular site of fusion.

CEACAM1 has been reported to interact with ATP1A1 in porcine cells (41). Since murine CEACAM1a, the natural receptor of MHV, is a homologue thereof, we investigated whether the positive effect of ATP1A1 on MHV infection is somehow linked to MHV binding to CEACAM1a. We made use of a mutant of MHV (MHV-SRec (37)), which enters cells in a CEACAM1a-independent, but heparan sulfate-dependent manner. Transfection of HeLa or HeLa-mCC1a (expressing murine CEACAM1a) cells with three different siRNAs against ATP1A1 was followed by low MOI inoculation with GFP-expressing MHV-SRec (MHV-2aGFP-SRec) or MHV (MHV-EGFPM), respectively. After 8h of infection cells were collected and GFP expression was analyzed by fluorescence-activated cell sorting (FACS). As controls siRNA silencing GFP and negative-control siRNA were used. Infection with MHV-SRec of cells lacking the MHV receptor was reduced to the same extent as MHV infection of receptor-expressing cells by all three siRNAs targeting ATP1A1 (fig. 3B). These results indicate that, irrespective of the entry receptor, infection with MHV depends on ATP1A1.

Nanomolar concentrations of CTSs inhibit infection with CoVs and VSV, but not with IAV.

High concentrations of CTSs are known to inhibit the ion-pumping function of Na^+,K^+-ATPase (42-44). However, recent research has revealed that CTSs, in particular ouabain and bufalin, can trigger various signal transduction pathways mediated by Na^+,K^+-ATPase (14, 16-21, 45, 46) at much lower concentrations. In view of the critical role of ATP1A1 on infection of MHV and FIPV, we investigated to what extent CTSs affect infection of CoVs. Therefore, HeLa cells (MHV, FIPV [FIPV-H], VSV and IAV), Huh-7 cells (MERS-CoV) and feline FCWF cells (FIPV [FIPV-F]) were treated with ouabain or bufalin at high or low concentrations for 30 min and then inoculated with the indicated viruses in the presence of the drugs, after which the CTSs were kept present until cells were lysed or fixed. CTSs were also added to cells at 2h post infection (hpi) to assess the effects of these drugs on post-entry steps. At the indicated time points, cells were lysed or fixed and luciferase expression levels or number of virus-infected cells determined. Addition of relatively high concentrations of ouabain (250nM) or bufalin (50nM) had severe negative effects on infection with all viruses tested, both when added prior to or after inoculation (data not shown). Also translation of transfected synthetic, capped reporter mRNA was inhibited at these high concentrations (data not shown). Addition of low amounts of ouabain (50nM) or bufalin (10-15nM) inhibited infection with MHV, FIPV, MERS-CoV, and VSV, but only when added prior to inoculation. Infection was not affected when the drugs were added at 2 hpi. Infection with IAV was not affected by the addition of low concentrations of ouabain or bufalin (fig. 4A and 4B). These results show that low concentrations of CTSs inhibit infection with different CoVs, but not with IAV. CTSs most likely affect CoV infection during the entry stage, as no effect was observed when they were added after inoculation.

Effect of ouabain on MHV and VSV infection is linked to ATP1A1.

To confirm that the effect of ouabain on CoV infection is indeed linked to ATP1A1 we made use of the fact that rodent ATP1A1 encoded Na^+,K^+-ATPase is much more resistant to ouabain due to severely decreased binding of the drug to the protein caused by two amino acid mutations in the ectodomain (47). HeLa cells were transfected with plasmids encoding either human or murine ATP1A1. Transfected cells were pre-treated with nanomolar concentrations of ouabain and subsequently inoculated with luciferase-expressing MHV, IAV, or VSV in the presence of the drug. Ouabain was kept present until cells were lysed and luciferase expression levels were determined. As a control ouabain was also added to cells only from 2 hpi onwards. IAV infection was not affected by ouabain treatment, neither when human, nor when murine ATP1A1 was overexpressed (fig. 5). MHV and VSV infection of cells transfected with plasmid expressing human ATP1A1 was inhibited by ouabain. However, when the ouabain-insensitive murine ATP1A1 was overexpressed, the inhibitory effect of ouabain on infection was abolished (fig. 5). These results demonstrate that the inhibitory effect of ouabain on CoV infection is directly linked to ATP1A1.

CTSs decrease the fusion signal of MHV and VSV.

Next we investigated the inhibition of MHV infection by low levels of ouabain by performing an ouabain time-of-addition experiment (fig. 6A). Luciferase-expressing MHV was bound to HeLa-CC1a cells for 90 min on ice. Unbound virus was removed and cells were shifted to 37°C to allow infection. At the indicated time points cell culture media were replaced by warm, ouabain-containing medium. At 7 hpi cells were lysed and luciferase expression levels determined. Addition of ouabain only affected MHV infection when added during the first 2h of infection (fig. 6A), indicating that ouabain specifically inhibits MHV infection during entry.

To dissect which CoV entry step is affected by the addition of low concentrations of bufalin or ouabain we again made use of the replication-independent binding, internalization, and fusion assays. MHV-αN was bound to ΔM15-expressing cells that were pre-treated for 30 min with either ouabain or bufalin. Binding, internalization and fusion of MHV-αN were determined as described above. Binding and internalization of MHV did not appear to be affected by ouabain or bufalin treatment. However, the fusion signal of MHV was clearly reduced (fig. 6B). Very similar results were obtained for VSV (fig. 6C).

In addition, we analyzed whether the inhibition of MHV infection by ouabain is dependent on the nature of the entry receptor used or on the depth of MHV trafficking into the endo-lysosomal pathway. Therefore, HeLa-mCC1a and HeLa cells were inoculated with luciferase-expressing MHV (dependence on CEACAM1a and lysosomal trafficking), MHV-S2'FCS (fusion in early endosomes) or MHV-SRec (effect of receptor usage) in the presence of ouabain, after which the inhibitor was kept present until cell lysis. To control for any post entry effects of ouabain, the drug was also added and kept present only from 2h post inoculation onwards. As an additional control cells were treated with U18666A, which inhibits late endosome-to-lysosome trafficking (6, 48). Ouabain negatively affected infection with both MHV and MHV-S2'FCS (fig. 6D), indicating that it inhibits infection regardless of the intracellular site of fusion. In contrast, infection with MHV, but not with MHV-S2'FCS, was affected by U18666A. Also CEACAM1a-independent infection of MHV-SRec was inhibited to the same extent as MHV.

Ouabain inhibits virus entry at an early stage.

The replication-independent binding, internalization and fusion assays indicate that nanomolar levels of ouabain decrease the MHV fusion but not the internalization signal. To get more insight

into the inhibition of virus entry by ouabain, we analyzed whether MHV infection could recover during an overnight incubation upon removal of ouabain at 2 hpi. Our results (Fig. 7A) show that this is indeed the case. No inhibition of virus infection was observed when oubain was removed after virus inoculation. Virus infection was only inhibited when ouabain was kept present both during inoculation and the overnight incubation. This allowed us to study whether the block induced by ouabain inhibited entry of MHV upstream or downstream of the inhibitory effects of known inhibitors of virus entry (6, 34, 49). Cells were (mock-) treated with ouabain prior to and during inoculation with luciferase-expressing MHV. After removal of the inoculum, cells were incubated for another 16 h in the absence or presence of inhibitory agents known to affect MHV entry (6, 34). Subsequently cells were lysed and luciferase expression levels determined. Luciferase expression levels obtained after ouabain treatment prior to and during inoculation but not thereafter were set to 100% (fig. 7A; black bar). Overnight incubation in the presence of the cell-impermeable MHV fusion inhibitor peptide HR2 (50) did not inhibit MHV infection regardless of the absence or presence of ouabain during virus inoculation. However, virus infection was severely reduced when HR2 peptide was present during virus inoculation, confirming the ability of the HR2 peptide to inhibit entry (fig. 7B). Addition of inhibitors of dynamin-2 (Dyngo-4A; Dyngo), clathrin-mediated endocytosis (chlorpromazine; Chlopro), or endosomal maturation (bafilomycin A1; BafA1) all reduced infection with MHV when added after removal of ouabain (fig. 7C). The smaller inhibition observed after addition of BafA1 compared Dyngo-4A and chlorpromazine is in agreement with the reported inhibition of MHV entry by these compounds (6, 34). The inhibitors did not affect luciferase expression levels without prior incubation with ouabain, indicating that they do not affect MHV infection at post entry stages. These results indicate that ouabain inhibits infection with MHV upstream of the inhibitory effects of Dyngo, Chlopro and BafA1.

MHV particles remain associated close to the cell surface.

To confirm and visualize the early block in infection by ouabain, MHV covalently labeled with DyLight 488 (MHV-DL488; (6)) was bound to ouabain- or mock-treated cells for 90 min at MOI=20 on ice. After removal of unbound virus particles, cells were incubated for 90 min at 37°C in the presence or absence of ouabain. Cells were then fixed and analyzed by confocal microscopy. The contours of the cells were visualized using phalloidin, which stains the actin cytoskeleton. In mock-treated cells, relatively few fluorescent virions were visible inside the cells (fig. 8A, upper panel). On the other hand, in ouabain-treated cells a larger number of virions were observed which appeared however to remain associated close to the cell surface (fig. 8A, lower panel), in agreement with ouabain inhibiting virus entry at an early stage. The larger number of virions observed in the presence of ouabain is probably explained by the inhibition of virus uptake and subsequent trafficking of virus particles to lysosomes where they fuse and/or are broken down (6).

To assess whether also for VSV the block in infection is caused by an early entry block, we made use of the ability of VSV to bypass the endocytic uptake route when exposed to a low extracellular pH upon binding. Cells were pre-treated with 50nM ouabain. Cells were inoculated with luciferase-expressing VSV at MOI=0.1 in presence of 50nM Ouabain. 2hpi the inoculum was removed and unbound viruses washed away with ice-cold PBS. Cells were incubated for 2min in warm buffers at different pH (7.2, 6.5, 5.5, and 5.0) containing 50nM ouabain. Cells were subsequently incubated for another 7h in ouabaincontaining medium. Infection levels were determined by measuring the luciferase expression levels of cell lysates relative to those in mock-

450 treated cells. In agreement with VSV entry being inhibited by ouabain at an early stage, infection
451 could be rescued by a low-pH shock. (fig. 8B).
452
453 **Inhibitory effects of ouabain on CoV infection can be rescued by inhibitors of Src but not**
454 **PI3K.**
455 CoV infection is inhibited by low concentrations of CTSs known to trigger different Na^+,K^+-
456 ATPase-mediated signaling pathways but not to affect the ion-pump function (16-21). Two of the
457 main signaling pathways induced by CTSs and mediated through Na^+,K^+-ATPase involve the
458 activation of Src or PI3K (51). In order to elucidate whether these signaling pathways are
459 involved in the antiviral action of ouabain we (mock-)treated cells with ouabain alone or in
460 combination with either PI3K inhibitor wortmannin (52), Src inhibitor PP2 (53), or Na^+,K^+-
461 ATPase-mimetic Src-inhibitor peptide (pNaKtide). pNaKtide binds and inhibits the Na^+,K^+-
462 ATPase-interacting pool of Src (39). As a control cells were treated with the kinase inhibitors in
463 the absence of ouabain. The cells were inoculated with luciferase-expressing MHV, FIPV, or VSV
464 in the presence of the inhibitors, after which the drugs were kept present until cell lysis. To check
465 for inhibitory effects after virus entry, cells were also treated with inhibitors starting at 2 hpi. At
466 7 hpi cells were lysed and luciferase expression levels determined. For reasons unknown,
467 treatment of cells with wortmannin or PP2 during virus inoculation reduced MHV and VSV
468 infection by about 75% (fig. 9A and C), while the pNaKtide had a smaller negative effect. Infection
469 with FIPV was not affected by these inhibitors (fig. 9B). The much smaller inhibitory effect of
470 pNaKtide compared to PP2, can be explained by pNaKtide, in contrast to PP2, specifically
471 targeting the Na+,K+-ATPase-interacting pool of Src and having less (off target) effects compared
472 to PP2 (39, 54). MHV-, FIPV-, and VSV-driven luciferase expression levels were severely reduced
473 by ouabain when the drug was present during virus inoculation, yet not when added at 2 hpi

only, as observed earlier. The combined treatment with ouabain and wortmannin did not positively affect MHV, FIPV, or VSV infection compared to ouabain treatment alone. However, combined treatment of ouabain with PP2 or pNaKtide almost completely restored MHV, FIPV, and VSV infection to the levels observed after treatment with PP2 or pNaKtide alone (fig. 9A, B, and C). These results show that the negative effect of ouabain on the entry of MHV, FIPV, and VSV can be relieved by inhibition of Src.

480 **Discussion**

481 This study provides an extensive analysis of the role of the *ATP1A1*-encoded α1-subunit of
482 Na^+,K^+-ATPase in CoV infection. Using gene silencing we showed that ATP1A1 is important for
483 infection of cells with MHV and FIPV, but not IAV. Also entry of VSV was shown to depend on
484 ATP1A1. Lack of ATP1A1 was found not to affect MHV binding to cells and did not appear to
485 inhibit endosomal uptake, although fusion with cellular membranes was reduced. Consistently,
486 nanomolar concentrations of CTSs inhibited infection of cells with MHV, FIPV and MERS-CoV,
487 when the compounds were present during virus entry. Similar results were obtained with VSV,
488 but not with IAV. CTSs were shown to inhibit entry of MHV at an early stage, resulting in the
489 accumulation of virions close to the cell surface and as a consequence in reduced fusion. Viral
490 RNA replication *per se* was not affected by these compounds at the concentrations used. In
491 agreement with low concentrations of CTSs not affecting the ion transport function of Na^+,K^+-
492 ATPase (16-21), the anti-coronaviral effect could be relieved by the addition of inhibitors of Src
493 kinases, indicating that Src signaling mediated via ATP1A1 plays a crucial role in the inhibition of
494 infection with CoVs.
495
496 Knockdown of ATP1A1 or additions of low concentrations of CTSs inhibit CoV and VSV infection
497 during the virus entry stage, as we could demonstrate using our recently developed replication-
498 independent entry assays (34). CoV and VSV replication was not affected as revealed by adding
499 the CTSs after inoculation. Inhibition of MHV was found to be independent of the particular virus
500 receptor being used by the virus, despite the reported interaction between CEACAM1 and
501 ATP1A1 (41). This is in line with FIPV and MERS-CoV being similarly inhibited while using
502 entirely different entry receptors (55, 56). FIPV on the one and MHV and MERS-CoV on the other

hand belong to the α- and β-CoV genera, respectively, suggesting that CTSs may function as pan-CoV inhibitors.

Interpreting our combined results, we developed the model shown in figure 10. In this model, two elements are addressed. First, it recapitulates the early stage of CoV entry as we and others have described (6, 57-60): uptake of CoV in a pre-endosome that pinches off to form an early endosome. Based on our data we propose a model in which the uptake of MHV particles is arrested in pre-endosomal structures by transfection of siRNAs targeting ATP1A1 or by the addition of CTSs, rather than having a direct effect on virus-cell fusion. This model explains the apparent paradoxical observations that internalization of MHV particles was not affected by ATP1A1 interference, while on the other hand, ouabain was shown to inhibit a very early step in MHV entry, upstream of the inhibitory effect of compounds affecting dynamin-2 and/or clathrin-mediated endocytosis (6). The internalization assay depends on the removal of cell surface-bound virions by proteases. The lack of internalization inhibition observed with this assay can be explained by MHV particles accumulating in pre-endosomal invaginations, which are not accessible by the membrane-impermeable protease in the presence of ouabain. In agreement with this model, we previously showed that also the dynamin-2 inhibitor Dynasore has little effect on the internalization of MHV and VSV virions, while fusion was severely hampered (34). Also the inability of the membrane-impermeable inhibitory HR2 peptide to prevent MHV infection after ouabain wash-out can be explained by the inability of the HR2 compound to access the pre-endosomal structures. The inhibition of MHV entry by inhibitors of clathrin-mediated endocytosis after ouabain wash-out indicates that further internalization of the pre-endosomal invaginations is sensitive to these inhibitors. In agreement with our model, interference with the Na^+,K^+-ATPase (either by ATP1A1 knockdown or addition of CTSs) inhibited CoV entry,

527 regardless whether viruses fusing in early endosomes (MHV-2'FCS and MERS-CoV) or lysosomes
528 (MHV and FIPV) were used (6). These results indicate that interference with the ATP1A1 subunit
529 acts prior to the formation of early endosomes and does not result from a defect in endosome
530 maturation. Our model is supported by confocal microscopy analysis, which showed MHV
531 particles to accumulate close to the cell surface in the presence of ouabain. Like for the CoVs, also
532 entry of VSV, but not of IAV, was inhibited by ouabain. Apparently, treatment of cells with oubain
533 does not affect the low pH in the endosomes which is essential for entry of both IAV and VSV (61-
534 63). The ability to bypass the VSV entry block induced by ouabain by low-pH shock indicates that
535 fusion *per se* of VSV is not affected, but rather results from ouabain preventing uptake of VSV in
536 early endosomes where fusion can take place (49, 61, 62).
537
538 The second element represented in our model (fig. 10) addresses the mechanism by which
539 interference with the ATP1A1 subunit activity blocks CoV and VSV entry. Our results indicate that
540 CoV infection is inhibited by low concentrations of CTSs via Na^+,K^+-ATPase-mediated Src
541 signaling. CoV infection of HeLa cells expressing ouabain insensitive murine ATP1A1-encoded
542 α1-subunit (47) was unaffected by ouabain treatment. These results show that ouabain mediates
543 its antiviral effect via the α1-subunit and not via an off-target effect, in agreement with the
544 literature (reviewed in (13, 14)). Ample evidence exists in the literature demonstrating that
545 nanomolar concentrations of CTSs induce α1-subunit-mediated signaling pathways, including the
546 activation of Src. At these concentrations, ouabain binding to the α1-subunit triggers a
547 conformational change in this subunit, which results in release of Src from Na^+,K^+-ATPase and its
548 concomitant activation (16-18, 22-28). The alleviation of inhibition of CoV infection by ouabain
549 with two chemically different Src inhibitors, PP2 and pNaKtide, but not by an inhibitor of PI3K,
550 shows that the activation of Src via the α1-subunit is the inhibitory mode of action of this

compound on CoV infection. In agreement with the inhibitory effect of Na^+,K^+-ATPase-mediated Src signaling on CoV infection, also gene silencing of ATP1A1 has been shown to result in activation of Src (20, 39, 64).

We speculate that ATP1A1-mediated Src signalling somehow interferes with clathrin-mediated uptake of CoVs and VSV. Similar to MHV (6, 57-60) and VSV (49, 61), also MERS-CoV and FIPV appear to be taken up via clathrin-mediated endocytosis as infection with these viruses is inhibited by chlorpromazine in a dose-dependent manner ((65) and unpublished results), although FIPV has also been reported to enter monocytes via a clathrin- and caveolae-independent endocytic pathway (66). An explanation for the lack of inhibition of IAV could be that this virus is able to enter cells via multiple fully redundant endocytic routes (63, 67-70). ATP1A1-mediated Src signaling has been shown to induce phosphorylation of dynamin-2 and caveolar endocytosis (64, 71). However, it is not yet clear how ATP1A1-mediated Src signaling could interfere with clathrin-mediated entry of CoVs and VSV. Other studies have shown the importance of Src-mediated phosphorylation of dynamin-2 in clathrin- as well as caveolae-mediated endocytic uptake of cargo (72-74). For reoviruses, which are probably taken up via clathrin-mediated endocytosis, Src phosphorylation has also been shown to mediate endocytic sorting of these viruses, internalization of reovirus virions, however, was not affected by inhibition of Src signaling (75). Spatiotemporal compartmentalization and regulation of Src signaling may be an important determinant of the specificity of Src signaling and of the different biological outcomes observed (76, 77).

Inhibition of infection by CTSs has been reported earlier for several other viruses including Sindbis virus (78), Sendai virus (79), Semliki Forest virus (80), several herpes viruses (81), and

Journal of Virology

PRRSV (82). Most of these studies, however, employed relatively high concentrations of the CTSs (micromolar range) which inhibit the Na^+,K^+-ATPase pump function and affect intracellular ion-concentrations (83, 84). In the present study, the low levels of CTSs did not affect infection with IAV. However, at high concentrations infections by CoVs, VSV and IAVs were inhibited also when the compounds were only present after virus entry. This more general inhibitory effect at these concentrations may result from side effects of the drugs such as, for instance, inhibition of mRNA translation (data not shown). Indeed, intracellular levels of Na+ and K+ have been implicated previously in the regulation of cellular protein synthesis (85, 86). Interestingly, for human cytomegalovirus, low nanomolar concentrations of ouabain were shown to inhibit an early step in the infection cycle of this virus prior to DNA replication, but following binding to cellular receptors, suggesting that also for this virus entry may be impaired (81).

Ouabain and several other CTSs are FDA-approved compounds. Targeting host factors using FDA-approved compounds to combat viral infections is certainly attractive. Drugs targeting host-, rather than viral factors may lower the probability of generating drug-resistant viral variants since mutation of the drug target is not possible. In addition, the repurposing of FDA-approved compounds may enable relatively fast clinical application. Elucidation of the action mechanism of the anti-viral compounds as exemplified here by the anti-CoV and -VSV effect of low concentrations of CTSs may aid the development and design of new compounds with improved therapeutic efficacy and less side effects.

Acknowledgments

We would like to thank Zijian Xie, Marshall University, Institute of Interdisciplinary Research, Huntington, US-VA, for providing us with pNaKtide. This work was supported by the EU 7th Framework Programme (Virus Entry, project 235649, P.J.M.R) and by a Utrecht University High potential grant to C.A.M.d.H.

603 **References**

604

605 1. **Alvarez-Salas LM.** 2008. Nucleic acids as therapeutic agents. Current topics in medicinal
606 chemistry **8:**1379-1404.
607 2. **Hirsch AJ.** 2010. The use of RNAi-based screens to identify host proteins involved in viral
608 replication. Future microbiology **5:**303-311.
609 3. **Pauli I, Timmers LF, Caceres RA, Soares MB, de Azevedo WF, Jr.** 2008. In silico and in
610 vitro: identifying new drugs. Current drug targets **9:**1054-1061.
611 4. **Peiris JS, Lai ST, Poon LL, Guan Y, Yam LY, Lim W, Nicholls J, Yee WK, Yan WW,**
612 **Cheung MT, Cheng VC, Chan KH, Tsang DN, Yung RW, Ng TK, Yuen KY.** 2003.
613 Coronavirus as a possible cause of severe acute respiratory syndrome. Lancet **361:**1319-
614 1325.
615 5. **Zaki AM, van Boheemen S, Bestebroer TM, Osterhaus AD, Fouchier RA.** 2012.
616 Isolation of a novel coronavirus from a man with pneumonia in Saudi Arabia. N Engl J Med
617 **367:**1814-1820.
618 6. **Burkard C, Verheije MH, Wicht O, van Kasteren SI, van Kuppeveld FJ, Haagmans BL,**
619 **Pelkmans L, Rottier PJ, Bosch BJ, de Haan CA.** 2014. Coronavirus Cell Entry Occurs
620 through the Endo-/Lysosomal Pathway in a Proteolysis-Dependent Manner. PLoS
621 pathogens **10:**e1004502.
622 7. **Hagemeijer MC, Rottier PJ, de Haan CA.** 2012. Biogenesis and dynamics of the
623 coronavirus replicative structures. Viruses **4:**3245-3269.
624 8. **de Haan CA, Rottier PJ.** 2005. Molecular interactions in the assembly of coronaviruses.
625 Advances in virus research **64:**165-230.
626 9. **Skou JC.** 2004. The identification of the sodium pump. Bioscience reports **24:**436-451.
627 10. **Kaplan JH.** 2002. Biochemistry of Na,K-ATPase. Annual review of biochemistry **71:**511-
628 535.
629 11. **Withering W.** 1785. An Account of the Foxglove and some of its Medical Uses With
630 Practical Remarks on Dropsy and Other Diseases.
631 12. **Schoner W, Scheiner-Bobis G.** 2007. Endogenous and exogenous cardiac glycosides and
632 their mechanisms of action. American journal of cardiovascular drugs : drugs, devices, and
633 other interventions **7:**173-189.
634 13. **Reinhard L, Tidow H, Clausen MJ, Nissen P.** 2013. Na(+),K (+)-ATPase as a docking
635 station: protein-protein complexes of the Na(+),K (+)-ATPase. Cellular and molecular life
636 sciences : CMLS **70:**205-222.
637 14. **Aperia A.** 2007. New roles for an old enzyme: Na,K-ATPase emerges as an interesting
638 drug target. Journal of internal medicine **261:**44-52.
639 15. **Karpova LV, Bulygina ER, Boldyrev AA.** 2010. Different neuronal Na(+)/K(+)-ATPase
640 isoforms are involved in diverse signaling pathways. Cell biochemistry and function
641 **28:**135-141.
642 16. **Aizman O, Uhlen P, Lal M, Brismar H, Aperia A.** 2001. Ouabain, a steroid hormone that
643 signals with slow calcium oscillations. Proceedings of the National Academy of Sciences of
644 the United States of America **98:**13420-13424.
645 17. **Haas M, Askari A, Xie Z.** 2000. Involvement of Src and epidermal growth factor receptor
646 in the signal-transducing function of Na+/K+-ATPase. The Journal of biological chemistry
647 **275:**27832-27837.

18. **Mohammadi K, Kometiani P, Xie Z, Askari A.** 2001. Role of protein kinase C in the signal pathways that link Na+/K+-ATPase to ERK1/2. The Journal of biological chemistry **276:**42050-42056.
19. **Su CT, Hsu JT, Hsieh HP, Lin PH, Chen TC, Kao CL, Lee CN, Chang SY.** 2008. Anti-HSV activity of digitoxin and its possible mechanisms. Antiviral research **79:**62-70.
20. **Tian J, Cai T, Yuan Z, Wang H, Liu L, Haas M, Maksimova E, Huang XY, Xie ZJ.** 2006. Binding of Src to Na+/K+-ATPase forms a functional signaling complex. Molecular biology of the cell **17:**317-326.
21. **Tian J, Gong X, Xie Z.** 2001. Signal-transducing function of Na+-K+-ATPase is essential for ouabain's effect on [Ca2+]i in rat cardiac myocytes. American journal of physiology. Heart and circulatory physiology **281:**H1899-1907.
22. **Barwe SP, Anilkumar G, Moon SY, Zheng Y, Whitelegge JP, Rajasekaran SA, Rajasekaran AK.** 2005. Novel role for Na,K-ATPase in phosphatidylinositol 3-kinase signaling and suppression of cell motility. Molecular biology of the cell **16:**1082-1094.
23. **Belusa R, Wang ZM, Matsubara T, Sahlgren B, Dulubova I, Nairn AC, Ruoslahti E, Greengard P, Aperia A.** 1997. Mutation of the protein kinase C phosphorylation site on rat alpha1 Na+,K+-ATPase alters regulation of intracellular Na+ and pH and influences cell shape and adhesiveness. The Journal of biological chemistry **272:**20179-20184.
24. **Contreras RG, Shoshani L, Flores-Maldonado C, Lazaro A, Cereijido M.** 1999. Relationship between Na(+),K(+)-ATPase and cell attachment. Journal of cell science **112 (Pt 23):**4223-4232.
25. **Li J, Zelenin S, Aperia A, Aizman O.** 2006. Low doses of ouabain protect from serum deprivation-triggered apoptosis and stimulate kidney cell proliferation via activation of NF-kappaB. Journal of the American Society of Nephrology : JASN **17:**1848-1857.
26. **Kometiani P, Li J, Gnudi L, Kahn BB, Askari A, Xie Z.** 1998. Multiple signal transduction pathways link Na+/K+-ATPase to growth-related genes in cardiac myocytes. The roles of Ras and mitogen-activated protein kinases. The Journal of biological chemistry **273:**15249-15256.
27. **Liu J, Tian J, Haas M, Shapiro JI, Askari A, Xie Z.** 2000. Ouabain interaction with cardiac Na+/K+-ATPase initiates signal cascades independent of changes in intracellular Na+ and Ca2+ concentrations. The Journal of biological chemistry **275:**27838-27844.
28. **Miyakawa-Naito A, Uhlen P, Lal M, Aizman O, Mikoshiba K, Brismar H, Zelenin S, Aperia A.** 2003. Cell signaling microdomain with Na,K-ATPase and inositol 1,4,5-trisphosphate receptor generates calcium oscillations. The Journal of biological chemistry **278:**50355-50361.
29. **Kuo L, Godeke GJ, Raamsman MJ, Masters PS, Rottier PJ.** 2000. Retargeting of coronavirus by substitution of the spike glycoprotein ectodomain: crossing the host cell species barrier. J Virol **74:**1393-1406.
30. **Konig R, Stertz S, Zhou Y, Inoue A, Hoffmann HH, Bhattacharyya S, Alamares JG, Tscherne DM, Ortigoza MB, Liang Y, Gao Q, Andrews SE, Bandyopadhyay S, De Jesus P, Tu BP, Pache L, Shih C, Orth A, Bonamy G, Miraglia L, Ideker T, Garcia-Sastre A, Young JA, Palese P, Shaw ML, Chanda SK.** 2010. Human host factors required for influenza virus replication. Nature **463:**813-817.
31. **van Boheemen S, de Graaf M, Lauber C, Bestebroer TM, Raj VS, Zaki AM, Osterhaus AD, Haagmans BL, Gorbalenya AE, Snijder EJ, Fouchier RA.** 2012. Genomic characterization of a newly discovered coronavirus associated with acute respiratory distress syndrome in humans. mBio **3**.

32. **Tani H, Komoda Y, Matsuo E, Suzuki K, Hamamoto I, Yamashita T, Moriishi K, Fujiyama K, Kanto T, Hayashi N, Owsianka A, Patel AH, Whitt MA, Matsuura Y.** 2007. Replication-competent recombinant vesicular stomatitis virus encoding hepatitis C virus envelope proteins. Journal of virology **81:**8601-8612.
33. **Wurdinger T, Verheije MH, Raaben M, Bosch BJ, de Haan CA, van Beusechem VW, Rottier PJ, Gerritsen WR.** 2005. Targeting non-human coronaviruses to human cancer cells using a bispecific single-chain antibody. Gene therapy **12:**1394-1404.
34. **Burkard C, Bloyet LM, Wicht O, van Kuppeveld FJ, Rottier PJ, de Haan CA, Bosch BJ.** 2014. Dissecting Virus Entry: Replication-Independent Analysis of Virus Binding, Internalization, and Penetration Using Minimal Complementation of beta-Galactosidase. PloS one **9:**e101762.
35. **de Haan CA, van Genne L, Stoop JN, Volders H, Rottier PJ.** 2003. Coronaviruses as vectors: position dependence of foreign gene expression. Journal of virology **77:**11312-11323.
36. **de Haan CA, Haijema BJ, Boss D, Heuts FW, Rottier PJ.** 2005. Coronaviruses as vectors: stability of foreign gene expression. Journal of virology **79:**12742-12751.
37. **de Haan CA, Li Z, te Lintelo E, Bosch BJ, Haijema BJ, Rottier PJ.** 2005. Murine coronavirus with an extended host range uses heparan sulfate as an entry receptor. Journal of virology **79:**14451-14456.
38. **Bosch BJ, van der Zee R, de Haan CA, Rottier PJ.** 2003. The coronavirus spike protein is a class I virus fusion protein: structural and functional characterization of the fusion core complex. J Virol **77:**8801-8811.
39. **Li Z, Cai T, Tian J, Xie JX, Zhao X, Liu L, Shapiro JI, Xie Z.** 2009. NaKtide, a Na/K-ATPase-derived peptide Src inhibitor, antagonizes ouabain-activated signal transduction in cultured cells. The Journal of biological chemistry **284:**21066-21076.
40. **Langley KE, Villarejo MR, Fowler AV, Zamenhof PJ, Zabin I.** 1975. Molecular basis of beta-galactosidase alpha-complementation. Proceedings of the National Academy of Sciences of the United States of America **72:**1254-1257.
41. **Gupta S, Yan Y, Malhotra D, Liu J, Xie Z, Najjar SM, Shapiro JI.** 2012. Ouabain and insulin induce sodium pump endocytosis in renal epithelium. Hypertension **59:**665-672.
42. **Blaustein MP, Juhaszova M, Golovina VA.** 1998. The cellular mechanism of action of cardiotonic steroids: a new hypothesis. Clinical and experimental hypertension **20:**691-703.
43. **Dvela M, Rosen H, Feldmann T, Nesher M, Lichtstein D.** 2007. Diverse biological responses to different cardiotonic steroids. Pathophysiology : the official journal of the International Society for Pathophysiology / ISP **14:**159-166.
44. **Wasserstrom JA, Aistrup GL.** 2005. Digitalis: new actions for an old drug. American journal of physiology. Heart and circulatory physiology **289:**H1781-1793.
45. **Kurosawa M, Numazawa S, Tani Y, Yoshida T.** 2000. ERK signaling mediates the induction of inflammatory cytokines by bufalin in human monocytic cells. American journal of physiology. Cell physiology **278:**C500-508.
46. **Watabe M, Masuda Y, Nakajo S, Yoshida T, Kuroiwa Y, Nakaya K.** 1996. The cooperative interaction of two different signaling pathways in response to bufalin induces apoptosis in human leukemia U937 cells. The Journal of biological chemistry **271:**14067-14072.
47. **Jewell-Motz EA, Lingrel JB.** 1993. Site-directed mutagenesis of the Na,K-ATPase: consequences of substitutions of negatively-charged amino acids localized in the transmembrane domains. Biochemistry **32:**13523-13530.

48. **Huynh KK, Gershenzon E, Grinstein S.** 2008. Cholesterol accumulation by macrophages impairs phagosome maturation. The Journal of biological chemistry **283:**35745-35755.
49. **Johannsdottir HK, Mancini R, Kartenbeck J, Amato L, Helenius A.** 2009. Host cell factors and functions involved in vesicular stomatitis virus entry. Journal of virology **83:**440-453.
50. **Bosch BJ, van der Zee R, de Haan CA, Rottier PJ.** 2003. The coronavirus spike protein is a class I virus fusion protein: structural and functional characterization of the fusion core complex. Journal of virology **77:**8801-8811.
51. **Liu J, Xie ZJ.** 2010. The sodium pump and cardiotonic steroids-induced signal transduction protein kinases and calcium-signaling microdomain in regulation of transporter trafficking. Biochimica et biophysica acta **1802:**1237-1245.
52. **Yano H, Nakanishi S, Kimura K, Hanai N, Saitoh Y, Fukui Y, Nonomura Y, Matsuda Y.** 1993. Inhibition of histamine secretion by wortmannin through the blockade of phosphatidylinositol 3-kinase in RBL-2H3 cells. The Journal of biological chemistry **268:**25846-25856.
53. **Hanke JH, Gardner JP, Dow RL, Changelian PS, Brissette WH, Weringer EJ, Pollok BA, Connelly PA.** 1996. Discovery of a novel, potent, and Src family-selective tyrosine kinase inhibitor. Study of Lck- and FynT-dependent T cell activation. The Journal of biological chemistry **271:**695-701.
54. **Brandvold KR, Steffey ME, Fox CC, Soellner MB.** 2012. Development of a highly selective c-Src kinase inhibitor. ACS chemical biology **7:**1393-1398.
55. **Raj VS, Mou H, Smits SL, Dekkers DH, Muller MA, Dijkman R, Muth D, Demmers JA, Zaki A, Fouchier RA, Thiel V, Drosten C, Rottier PJ, Osterhaus AD, Bosch BJ, Haagmans BL.** 2013. Dipeptidyl peptidase 4 is a functional receptor for the emerging human coronavirus-EMC. Nature **495:**251-254.
56. **Tresnan DB, Levis R, Holmes KV.** 1996. Feline aminopeptidase N serves as a receptor for feline, canine, porcine, and human coronaviruses in serogroup I. Journal of virology **70:**8669-8674.
57. **Eifart P, Ludwig K, Bottcher C, de Haan CA, Rottier PJ, Korte T, Herrmann A.** 2007. Role of endocytosis and low pH in murine hepatitis virus strain A59 cell entry. Journal of virology **81:**10758-10768.
58. **Qiu Z, Hingley ST, Simmons G, Yu C, Das Sarma J, Bates P, Weiss SR.** 2006. Endosomal proteolysis by cathepsins is necessary for murine coronavirus mouse hepatitis virus type 2 spike-mediated entry. Journal of virology **80:**5768-5776.
59. **Stauber R, Pfleiderera M, Siddell S.** 1993. Proteolytic cleavage of the murine coronavirus surface glycoprotein is not required for fusion activity. The Journal of general virology **74 (Pt 2):**183-191.
60. **Sturman LS, Ricard CS, Holmes KV.** 1985. Proteolytic cleavage of the E2 glycoprotein of murine coronavirus: activation of cell-fusing activity of virions by trypsin and separation of two different 90K cleavage fragments. Journal of virology **56:**904-911.
61. **White J, Matlin K, Helenius A.** 1981. Cell fusion by Semliki Forest, influenza, and vesicular stomatitis viruses. The Journal of cell biology **89:**674-679.
62. **Blumenthal R, Bali-Puri A, Walter A, Covell D, Eidelman O.** 1987. pH-dependent fusion of vesicular stomatitis virus with Vero cells. Measurement by dequenching of octadecyl rhodamine fluorescence. The Journal of biological chemistry **262:**13614-13619.
63. **Lakadamyali M, Rust MJ, Zhuang X.** 2004. Endocytosis of influenza viruses. Microbes and infection / Institut Pasteur **6:**929-936.

64. **Cai T, Wang H, Chen Y, Liu L, Gunning WT, Quintas LE, Xie ZJ.** 2008. Regulation of caveolin-1 membrane trafficking by the Na/K-ATPase. The Journal of cell biology **182:**1153-1169.
65. **de Wilde AH, Jochmans D, Posthuma CC, Zevenhoven-Dobbe JC, van Nieuwkoop S, Bestebroer TM, van den Hoogen BG, Neyts J, Snijder EJ.** 2014. Screening of an FDA-approved compound library identifies four small-molecule inhibitors of Middle East respiratory syndrome coronavirus replication in cell culture. Antimicrobial agents and chemotherapy.
66. **Van Hamme E, Dewerchin HL, Cornelissen E, Verhasselt B, Nauwynck HJ.** 2008. Clathrin- and caveolae-independent entry of feline infectious peritonitis virus in monocytes depends on dynamin. The Journal of general virology **89:**2147-2156.
67. **de Vries E, Tscherne DM, Wienholts MJ, Cobos-Jimenez V, Scholte F, Garcia-Sastre A, Rottier PJ, de Haan CA.** 2011. Dissection of the influenza A virus endocytic routes reveals macropinocytosis as an alternative entry pathway. PLoS pathogens **7:**e1001329.
68. **Matlin KS, Reggio H, Helenius A, Simons K.** 1981. Infectious entry pathway of influenza virus in a canine kidney cell line. The Journal of cell biology **91:**601-613.
69. **Patterson S, Oxford JS, Dourmashkin RR.** 1979. Studies on the mechanism of influenza virus entry into cells. The Journal of general virology **43:**223-229.
70. **Sieczkarski SB, Whittaker GR.** 2002. Influenza virus can enter and infect cells in the absence of clathrin-mediated endocytosis. Journal of virology **76:**10455-10464.
71. **Harris TL.** 2012. Ouabain Regulates Caveolin-1 Vesicle Trafficking by a Src-Dependent Mechanism. Ph.D. The University of Toledo, Ann Arbor.
72. **Cao H, Chen J, Krueger EW, McNiven MA.** 2010. SRC-mediated phosphorylation of dynamin and cortactin regulates the "constitutive" endocytosis of transferrin. Molecular and cellular biology **30:**781-792.
73. **Shajahan AN, Timblin BK, Sandoval R, Tiruppathi C, Malik AB, Minshall RD.** 2004. Role of Src-induced dynamin-2 phosphorylation in caveolae-mediated endocytosis in endothelial cells. The Journal of biological chemistry **279:**20392-20400.
74. **Ahn S, Maudsley S, Luttrell LM, Lefkowitz RJ, Daaka Y.** 1999. Src-mediated tyrosine phosphorylation of dynamin is required for beta2-adrenergic receptor internalization and mitogen-activated protein kinase signaling. The Journal of biological chemistry **274:**1185-1188.
75. **Mainou BA, Dermody TS.** 2011. Src kinase mediates productive endocytic sorting of reovirus during cell entry. Journal of virology **85:**3203-3213.
76. **Veracini L, Franco M, Boureux A, Simon V, Roche S, Benistant C.** 2005. Two functionally distinct pools of Src kinases for PDGF receptor signalling. Biochemical Society transactions **33:**1313-1315.
77. **Veracini L, Simon V, Richard V, Schraven B, Horejsi V, Roche S, Benistant C.** 2008. The Csk-binding protein PAG regulates PDGF-induced Src mitogenic signaling via GM1. The Journal of cell biology **182:**603-614.
78. **Mento SJ, Stollar V.** 1978. Effect of ouabain on sindbis virus replication in ouabain-sensitive and ouabain-resistant Aedes albopictus cells (Singh). Virology **87:**58-65.
79. **Nagai Y, Maeno K, Iinuma M, Yoshida T, Matsumoto T.** 1972. Inhibition of virus growth by ouabain: effect of ouabain on the growth of HVJ in chick embryo cells. Journal of virology **9:**234-243.
80. **Helenius A, Kielian M, Wellsteed J, Mellman I, Rudnick G.** 1985. Effects of monovalent cations on Semliki Forest virus entry into BHK-21 cells. The Journal of biological chemistry **260:**5691-5697.

81. **Kapoor A, Cai H, Forman M, He R, Shamay M, Arav-Boger R.** 2012. Human cytomegalovirus inhibition by cardiac glycosides: evidence for involvement of the HERG gene. Antimicrobial agents and chemotherapy **56:**4891-4899.

82. **Karuppannan AK, Wu KX, Qiang J, Chu JJ, Kwang J.** 2012. Natural compounds inhibiting the replication of Porcine reproductive and respiratory syndrome virus. Antiviral research **94:**188-194.

83. **Beuschlein F, Boulkroun S, Osswald A, Wieland T, Nielsen HN, Lichtenauer UD, Penton D, Schack VR, Amar L, Fischer E, Walther A, Tauber P, Schwarzmayr T, Diener S, Graf E, Allolio B, Samson-Couterie B, Benecke A, Quinkler M, Fallo F, Plouin PF, Mantero F, Meitinger T, Mulatero P, Jeunemaitre X, Warth R, Vilsen B, Zennaro MC, Strom TM, Reincke M.** 2013. Somatic mutations in ATP1A1 and ATP2B3 lead to aldosterone-producing adenomas and secondary hypertension. Nature genetics **45:**440-444, 444e441-442.

84. **Chang JT, Lowery LA, Sive H.** 2012. Multiple roles for the Na,K-ATPase subunits, Atp1a1 and Fxyd1, during brain ventricle development. Developmental biology **368:**312-322.

85. **Frugulhetti IC, Rebello MA.** 1989. Na+ and K+ concentration and regulation of protein synthesis in L-A9 and Aedes albopictus cells infected with Marituba virus (Bunyaviridae). The Journal of general virology **70 (Pt 12):**3493-3499.

86. **Pauw PG, Kaffer CR, Petersen RJ, Semerad SA, Williams DC.** 2000. Inhibition of myogenesis by ouabain: effect on protein synthesis. In vitro cellular & developmental biology. Animal **36:**133-138.

87. **Ye J, Chen S, Maniatis T.** 2011. Cardiac glycosides are potent inhibitors of interferon-beta gene expression. Nature chemical biology **7:**25-33.

862 **Figure Legends**

863 **Figure 1. RNAi-mediated downregulation of ATP1A1 affects MHV, FIPV, and VSV but not**
864 **IAV. A)** Effect of RNAi-mediated downregulation of ATP1A1 on MHV-ERLM, FIPV-RLuc, IAV-
865 RLuc, and VSV-FLuc. Gene silencing was performed using individual transfection of three
866 different siRNAs targeting ATP1A1 (ATP1A1-1-3) in HeLa cells expressing the appropriate virus
867 receptors. Negative siRNA (neg siRNA) was taken along as a control. Cells were infected with
868 luciferase expressing viruses at MOI=0.1 for 7h or overnight for IAV. Infection levels were
869 determined by assaying the luciferase activity in cell lysates relative to lysates of infected cells
870 that had been mock treated. Infection levels were corrected for cell number and viability as
871 determined by the Wst-1 assay. Error bars represent SEM, n=3*3. **B)** Confirmation of siRNA-
872 mediated reduction in mRNA levels. mRNA levels at 72h post transfection were measured by
873 qRT-PCR relative to mock-transfected cells. Expression levels were corrected for cell number and
874 viability as determined by the Wst-1 assay. Error bars represent SEM, n=3*3. **A,B)** Dotted lines
875 indicate the lower 95% confidence interval of negative siRNA controls or mock treatment,
876 respectively.

877

878 **Figure 2. Knockdown of ATP1A1 affects MHV and VSV fusion. A)** Effects of siRNA-mediated
879 gene silencing on viral binding, internalization, and fusion using replication-independent assays.
880 Three different siRNAs against ATP1A1 (ATP1A1-1-3) were transfected individually into HeLa-
881 mCC1a-ΔM15. Negative siRNA (neg siRNA) was taken along as a control. At 72h post transfection
882 MHV-αN was allowed to bind to the cells on ice at MOI=20 for 90 min. Unbound virus was
883 washed off. For the binding assay cells and viruses were subsequently lysed and
884 complementation of ΔM15 by αN was determined relative to mock-treated samples using Beta-
885 Glo substrate and a luminometer. For internalization and fusion assays the cells were warmed to

886 37°C and virus was allowed to enter cells for 60 and 100 min, respectively. To assay
887 internalization cell surface bound virus was removed using trypsin and cells and viruses
888 subsequently lysed. Complementation of ΔM15 by αN was determined relative to mock-treated
889 samples using Beta-Glo substrate and a luminometer. For the fusion assay cells were pre-loaded
890 with FDG by hypotonic shock before inoculation. Upon infection for 100 min cells were collected
891 and analyzed by FACS. Fusion was determined relative to the number of FIC-positive cells
892 observed upon mock treatment of infected cells. Error bars represent SEM, n=3*3 for binding and
893 internalization, n=3 for fusion. **B)** VSV fusion was determined as described in A using VSV-
894 ΔG/Luc-Gα. **A, B)** Dotted lines indicate the lower 95% confidence intervals of the mock
895 treatment.
896
897 **Figure 3. Knockdown of ATP1A1 inhibits infection with MHV independent of the**
898 **intracellular site of fusion or the receptor used.** Gene silencing was performed as described
899 in the legend to figure 1. **A)** Cells were infected with luciferase expressing MHV or MHV-S2'FCS at
900 MOI=0.1 for 7h. Infection levels were determined by assaying the luciferase activity in cell lysates
901 relative to lysates of infected cells that had been mock treated. Infection levels were corrected for
902 cell number and viability as determined by the Wst-1 assay. Error bars represent SEM, n=3*3. **B)**
903 Cells were infected with GFP expressing MHV or MHV-SRec at MOI=0.5 for 8h. Cells were
904 collected and virus replication and cell viability analyzed by FACS relative to mock-treated
905 samples. Negative siRNA and siRNA targeting GFP were taken along as controls. Error bars
906 represent SEM, n=3.
907
908 **Figure 4. Low levels of ouabain and bufalin affect entry of CoVs and VSV but not of IAV. A)**
909 HeLa (MHV, FIPV [FIPV-H], VSV and IAV), Huh7 (MERS-CoV), or FCWF (FIPV [FIPV-F]) cells were

inoculated with the indicated viruses at MOI=0.1 for 2h. Cells were treated with 50nM ouabain from 30 min prior (pre) or 2 h post (post) inoculation until 7h (MHV and FIPV), 8h (MERS-CoV) or 16h (IAV) post infection. Infection levels were determined by measuring the luciferase activity in cell lysates or by determining the number of infected cells (MERS-CoV) by immunocytochemistry relative to mock-treated cells. Error bars represent SEM, n=3*3. **B)** Effect of low doses of bufalin on MHV, FIPV, MERS-CoV, IAV, and VSV infection. Cells were infected and treated as described in A with 10nM bufalin instead of ouabain. Error bars represent SEM, n=3*3.

Figure 5. Effect of ouabain on virus entry is linked to ATP1A1-encoded α1-subunit. HeLa cells were transfected with plasmids expressing either human or murine derived ATP1A1 (hATP1A1 and mATP1A1, respectively). Cells were treated with 50nM ouabain from 30 min prior (pre) or from 2 h post (post) inoculation with luciferase expressing MHV, IAV, or VSV at MOI=0.1 until 7h (MHV & VSV) or 16h (IAV) post infection. Infection levels were determined by measuring the luciferase activity in cell lysates relative to that in lysates of mock-treated cells. Infection levels were corrected for cell number and viability as determined by the Wst-1 assay prior to infection. Error bars represent SEM, n=3*3.

Figure 6. Low levels of ouabain and bufalin prevent fusion of MHV and VSV. A) Time-of-addition experiment using 50nM ouabain. Luciferase expressing MHV was bound to HeLa-mCC1a cells at MOI=0.5 for 90 min on ice. Unbound virus was washed off and incubation continued at 37°C. At indicated time points medium was replaced by warm medium containing 50nM ouabain. Luciferase expression levels were determined relative to mock-treated cells. Error bars represent SEM, n=3. **B)** Binding, internalization, and fusion assays of MHV upon ouabain or bufalin treatment were performed as described in the legend to figure 2. HeLa-mCC1a-ΔM15 cells were

Journal of Virology

pre-treated with 50nM ouabain or 10nM bufalin. **C)** Binding, internalization, and fusion assays of VSV were performed using VSV-ΔG/Luc-Gα similarly as described for MHV in the legend to figure 2. **B & C)** Error bars represent SEM, n=3*3 for binding and internalization, n=3 for fusion. **D)** Effect of ouabain treatment on infection with MHV-SRec or MHV-S2'FCS. Cells were treated with ouabain as described in the legend to figure 5 and inoculated with luciferase expressing MHV, MHV-S2'FCS, or MHV-SRec at MOI=0.1. As a control cells were treated with U18666A. Infection levels were determined by measuring the luciferase expression levels in cells at 7h post infection relative to those in mock-treated cells. Error bars represent SEM, n=3*3.

Figure 7. Ouabain inhibits virus entry upstream of inhibitors of CME. A) The inhibitory effect of ouabain is not observed when the compound is removed after virus inoculation. Cells were (mock-)treated with 50nM ouabain (Ou) starting at 30 min prior to and during inoculation (indicated by 0-2h) and/or after removal of the inoculum (indicated by 2-18h). Cells were inoculated with luciferase expressing MHV at MOI=0.1. **B)** Virus infection is not inhibited when the fusion inhibitory peptide HR2 is added after removal of ouabain. Cells were (mock-)treated with the indicated compounds (ouabain [Ou] or HR2 peptide [HR2]) starting at 30 min prior to and during inoculation (indicated by 0-2h) and/or after removal of the inoculum (indicated by 2-18h). **C)** After the removal of ouabain, virus infection is inhibited by the addition of CME inhibitors. Cells were (mock-)treated with 50nM ouabain (Ou) starting at 30 min prior to and during inoculation (indicated by 0-2h). After removal of the inoculum the medium was replaced by drug containing medium (Dyngo; Dyngo-4A, Chlorpro; Chlorpromazine, and BafA1; Bafilomycin A1). **A-C)** After overnight infection cells were lysed and infection levels were determined by measuring the luciferase activity in cell lysates relative to control cells that were

only treated with ouabain prior to and during inoculation (Ou 0-2h only, black bar). Error bars represent SEM, n=3*3.

Figure 8. Ouabain inhibits virus entry at an early stage. A) MHV particles accumulate close to the cell surface in the presence of ouabain. Imaging of ouabain-treated cells inoculated with DyLight 488-labelled MHV by confocal microscopy. Cells were mock-treated (upper two rows) or treated with 50nM ouabain (lower two rows) throughout the experiment starting at 30 min prior to inoculation. MHV covalently labeled with DyLight 488 (MHV particles) was bound to cells at MOI=20 for 70 min on ice. Unbound virus was removed and cell-bound virus was allowed to infect at 37°C for 90 min. Cells were fixed, stained with DAPI (Nuclei) and Phalloidin (Actin), and analyzed by confocal microscopy. Single z-slices are shown. **B)** The inhibitory effect of ouabain on VSV entry can be bypassed by low-pH shock-induced fusion. Cells were pre-treated with 50nM ouabain. VSV-FLuc virus was bound to the pre-treated cells at MOI=0.3 in presence of 50nM ouabain on ice for 90 min. Unbound virus was removed and cells incubated for 2h at 37°C in presence of ouabain. At 2hpi the inoculum was removed and cells incubated for 2min with warm buffers at different pH (7.2, 6.5, 5.5, and 5.0), containing 50nM ouabain. Incubation at 37°C in ouabain containing medium was continued until 11hpi. Infection levels were determined by measuring the luciferase expression levels in cell lysate relative to those in mock-treated cells. Error bars represent SEM, n=3*3.

Figure 9. Inhibition of infection by ouabain is rescued by inhibition of Src. HeLa cells were inoculated with luciferase expressing MHV (**A**), FIPV (**B**), or VSV (**C**) at MOI=0.1 for 2h. Cells were (pre-)treated with 50nM ouabain (Ou), wortmannin (Wort), PP2, pNaKtide or a combination thereof as indicated from 30 min prior to (pre) or 2h post (post) inoculation. The drugs were

kept present until cell lysis at 7h post inoculation. Infection levels were determined by measuring the luciferase activity in lysates of drug-treated relative to mock-treated cells. Error bars represent SEM, n=3*3.

Figure 10. Model of the effect of ATP1A1 knockdown and CTSs treatment on entry of CoVs and VSV. siRNA-mediated gene silencing of *ATP1A1* encoding the α1-subunit of the Na+,K+-ATPase or treatment of cells with CTSs inhibits infection with CoVs and VSV at an early entry stage, resulting in reduced virus-cell fusion. In the presence of CTSs or after siRNA-mediated gene silencing of *ATP1A1*, virus particles accumulate in pre-endosomal invaginations that are not accessible for the membrane impermeable HR2 peptide or trypsin. For VSV, this block in entry can be bypassed by low-pH shock. Knockdown of ATP1A1 leads to release of an Na^+,K^+-ATPase-bound subset of Src, Src activation, and increased Src signaling (20, 39, 64). Ouabain binding to the α1-subunit subunit of Na^+,K^+-ATPase triggers a conformational change in this subunit, which also results in release of Src from Na^+,K^+-ATPase and its concomitant activation (20, 87). Activated Src induces yet unknown downstream signaling, which inhibits virus entry at an early stage upstream of the inhibitory effects of inhibitors of clathrin-mediated endocytosis.

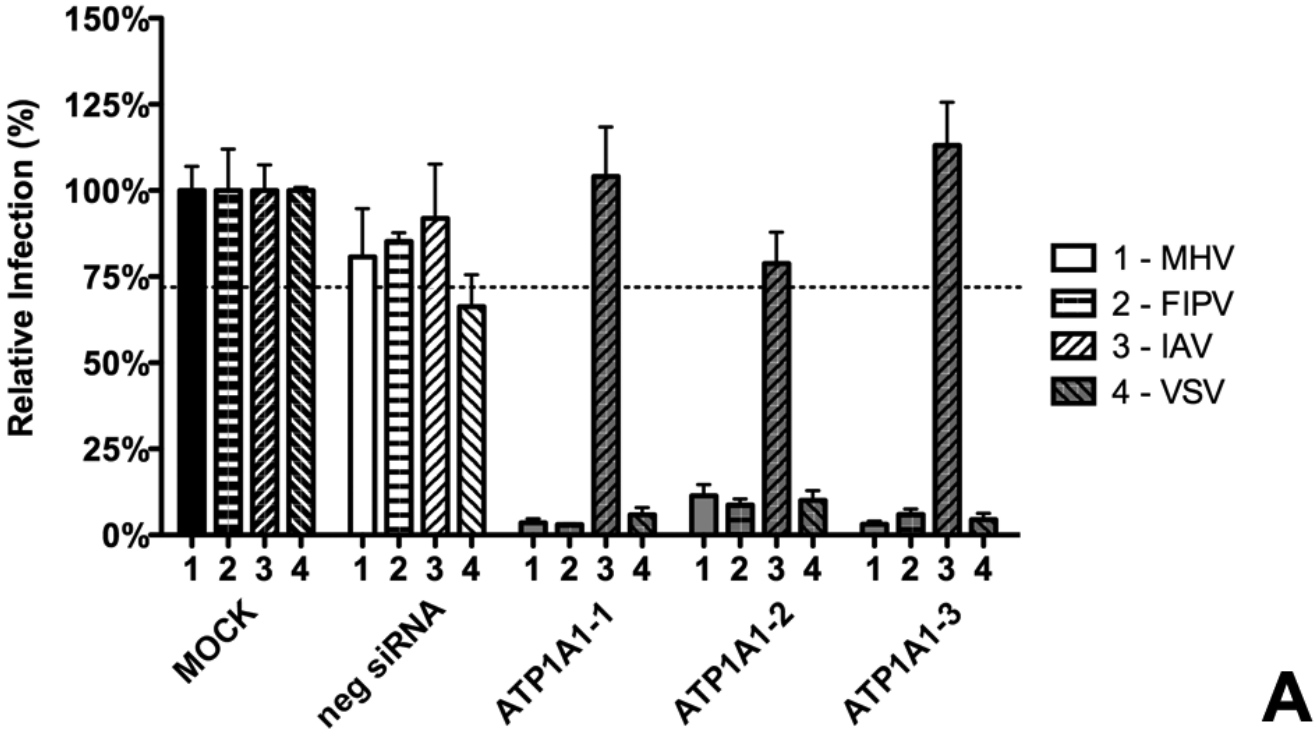

A

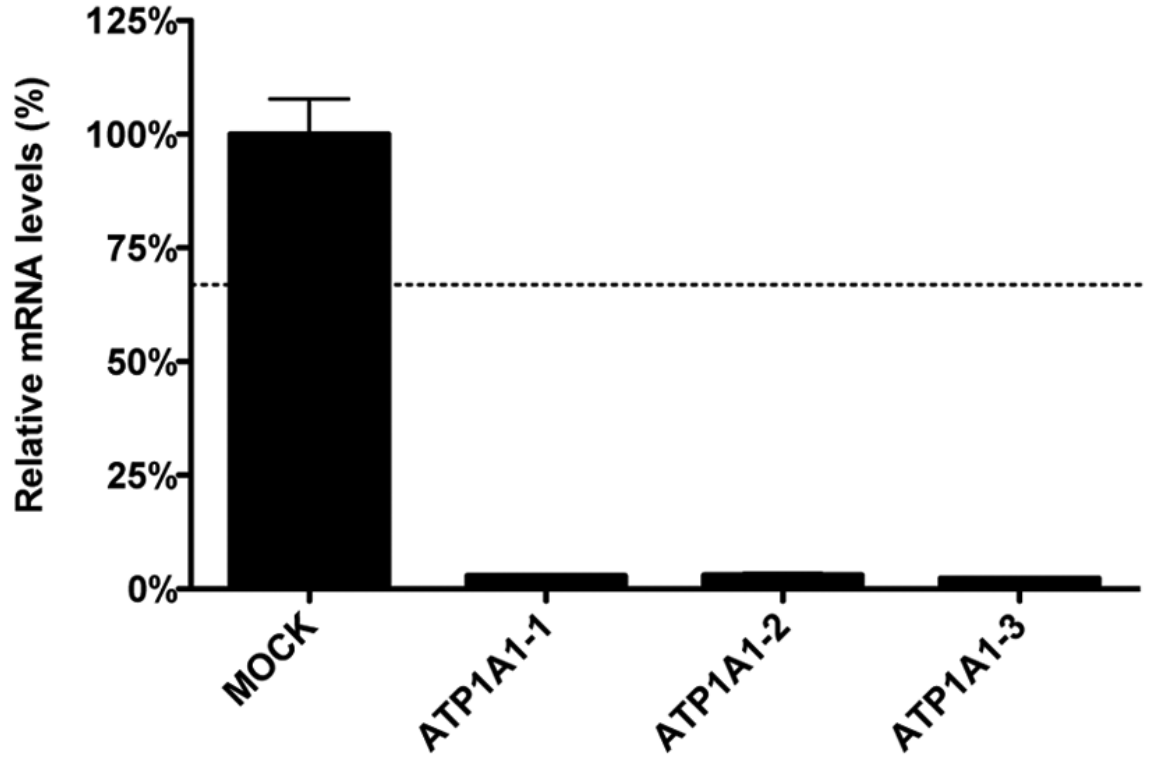

B

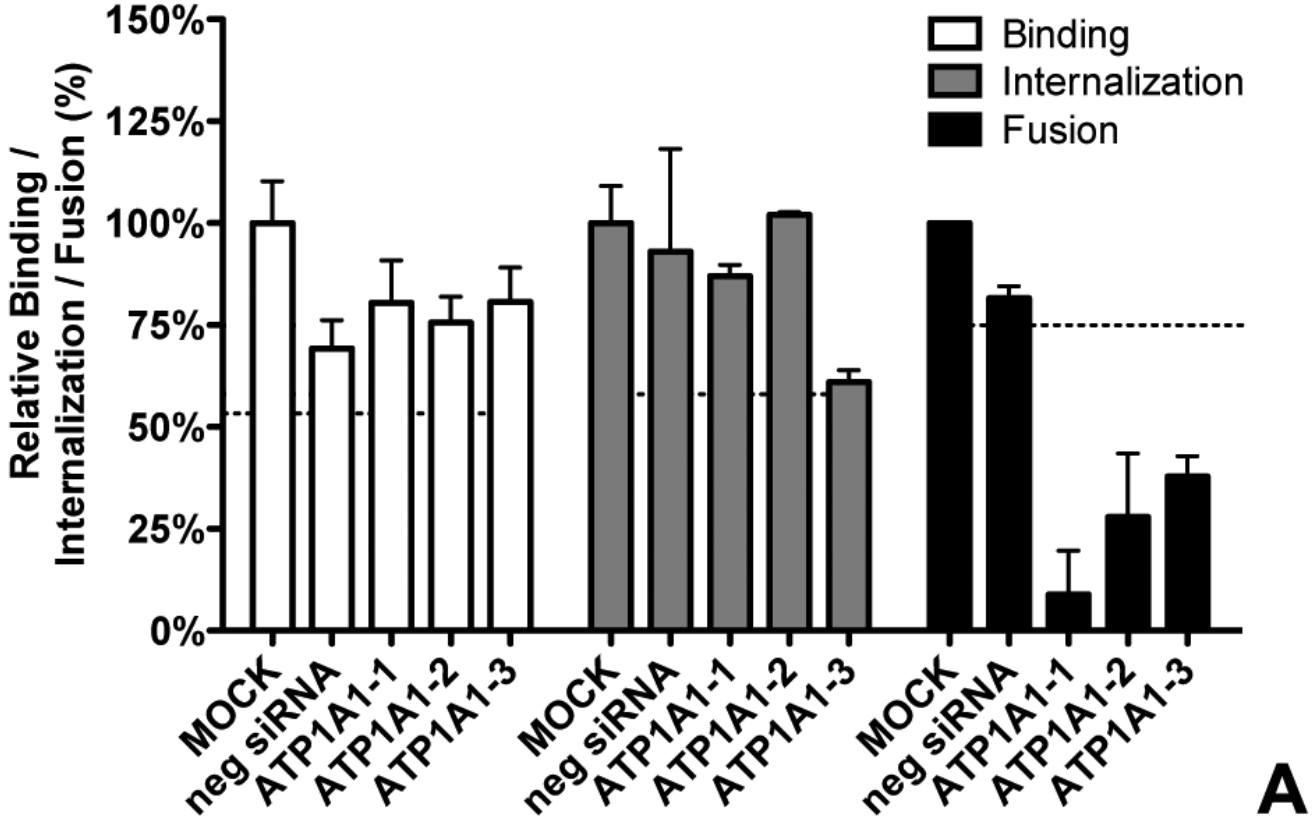

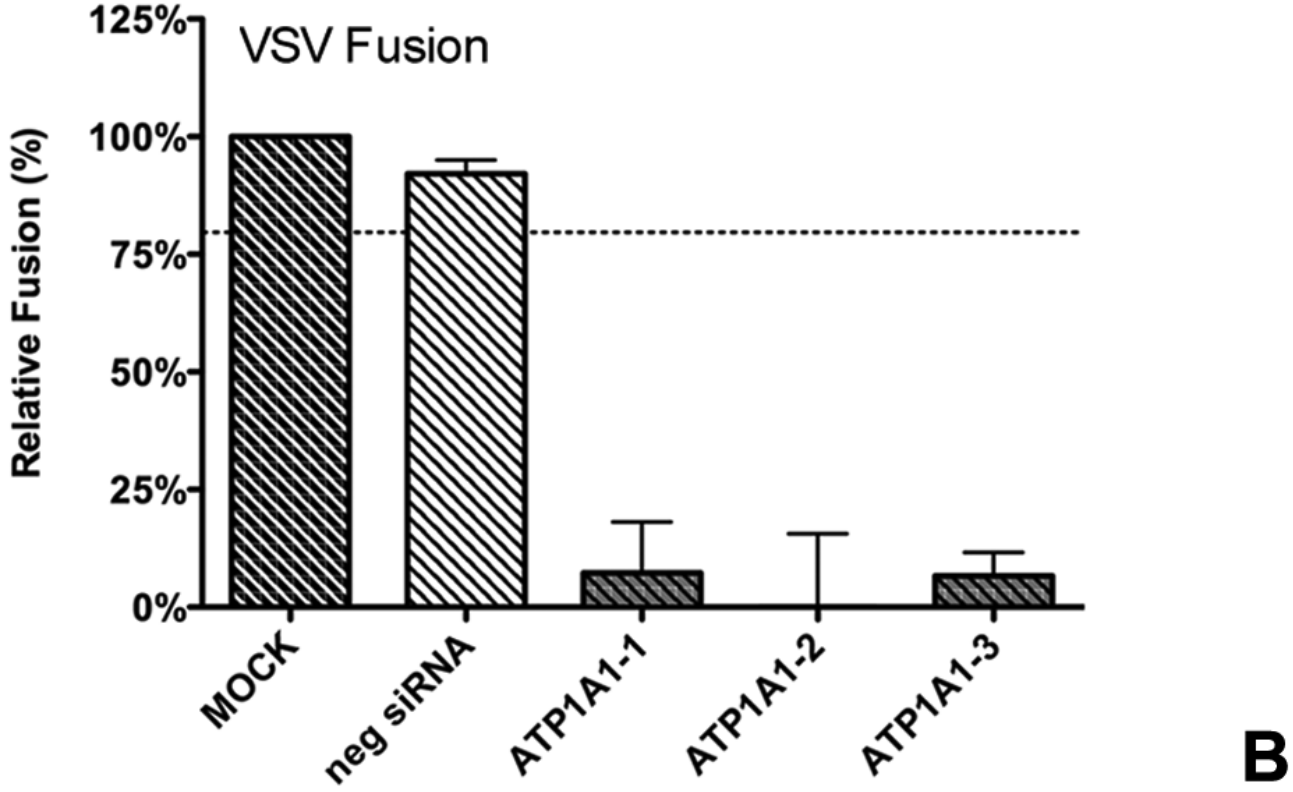

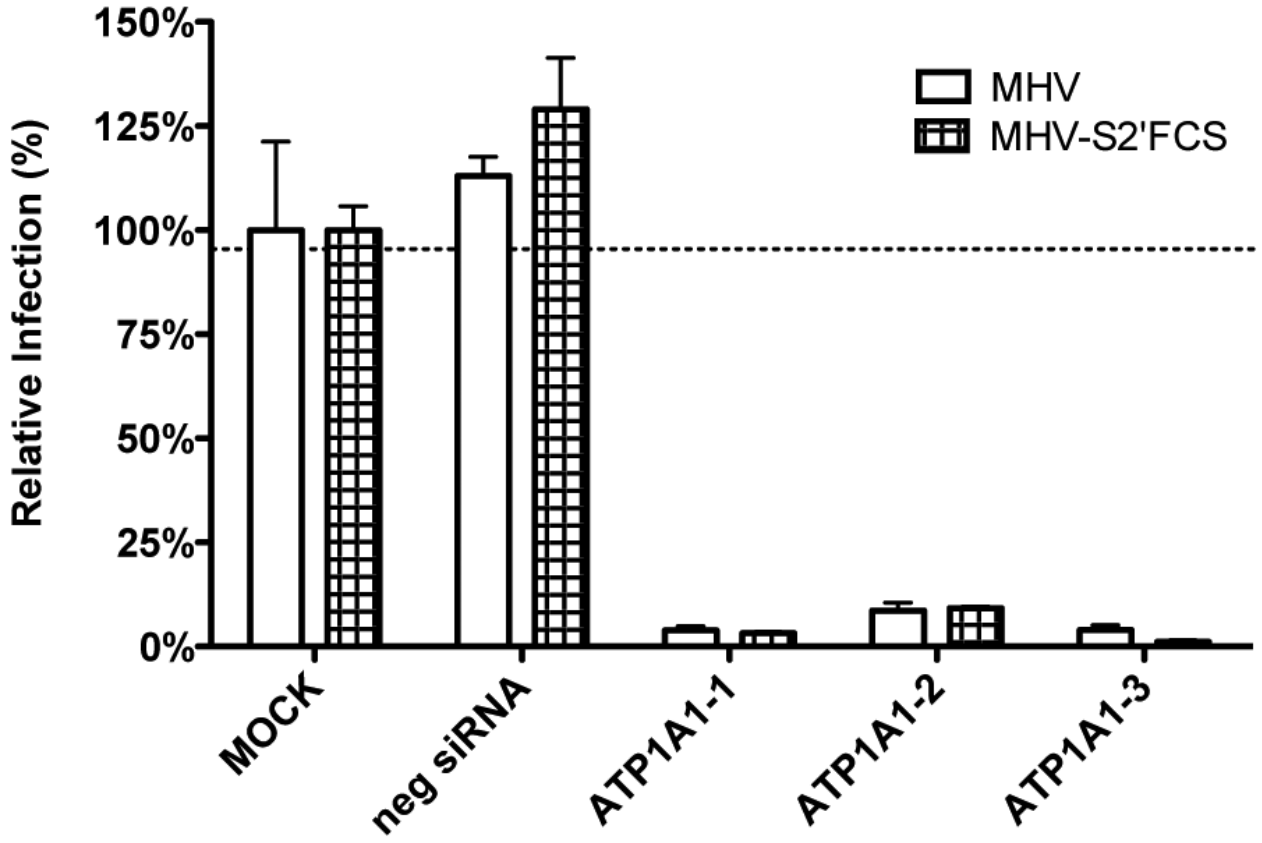

A

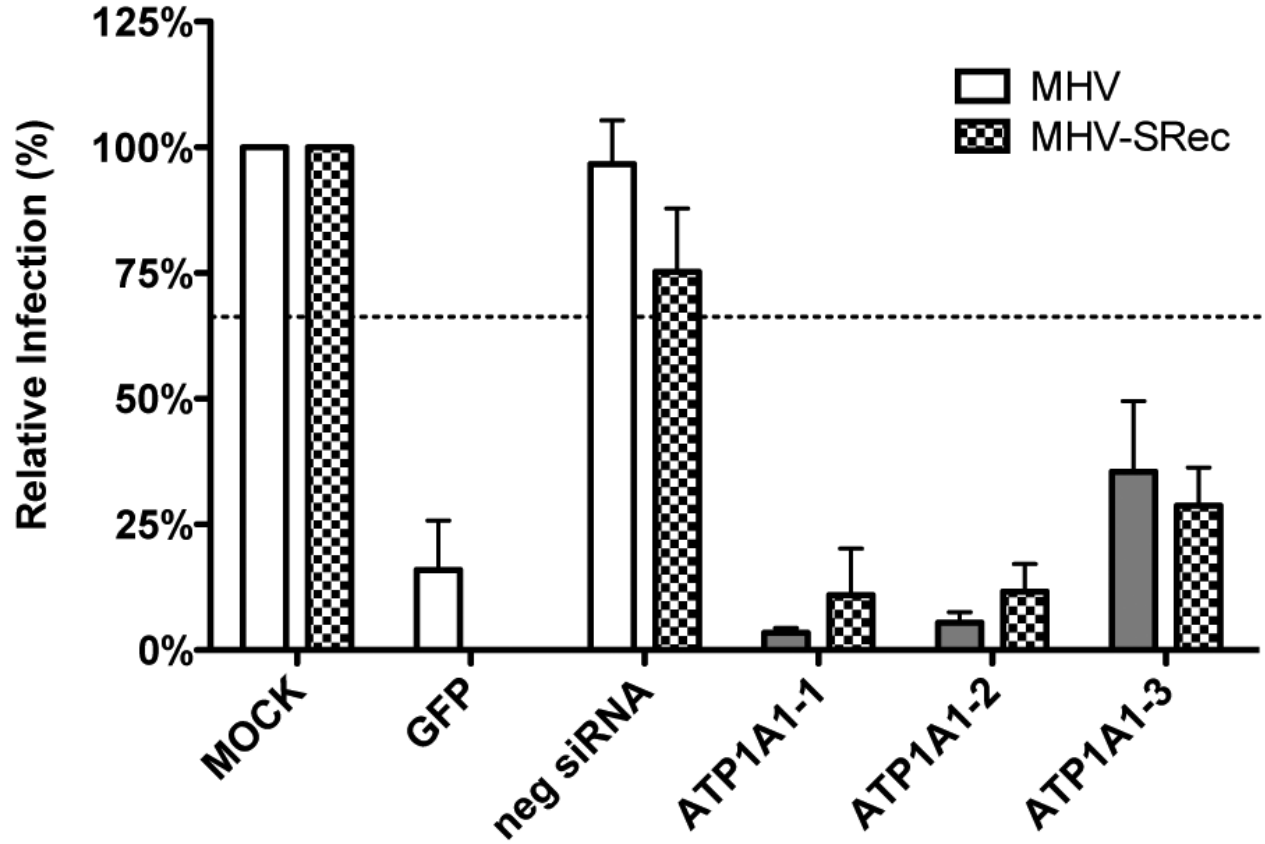

B

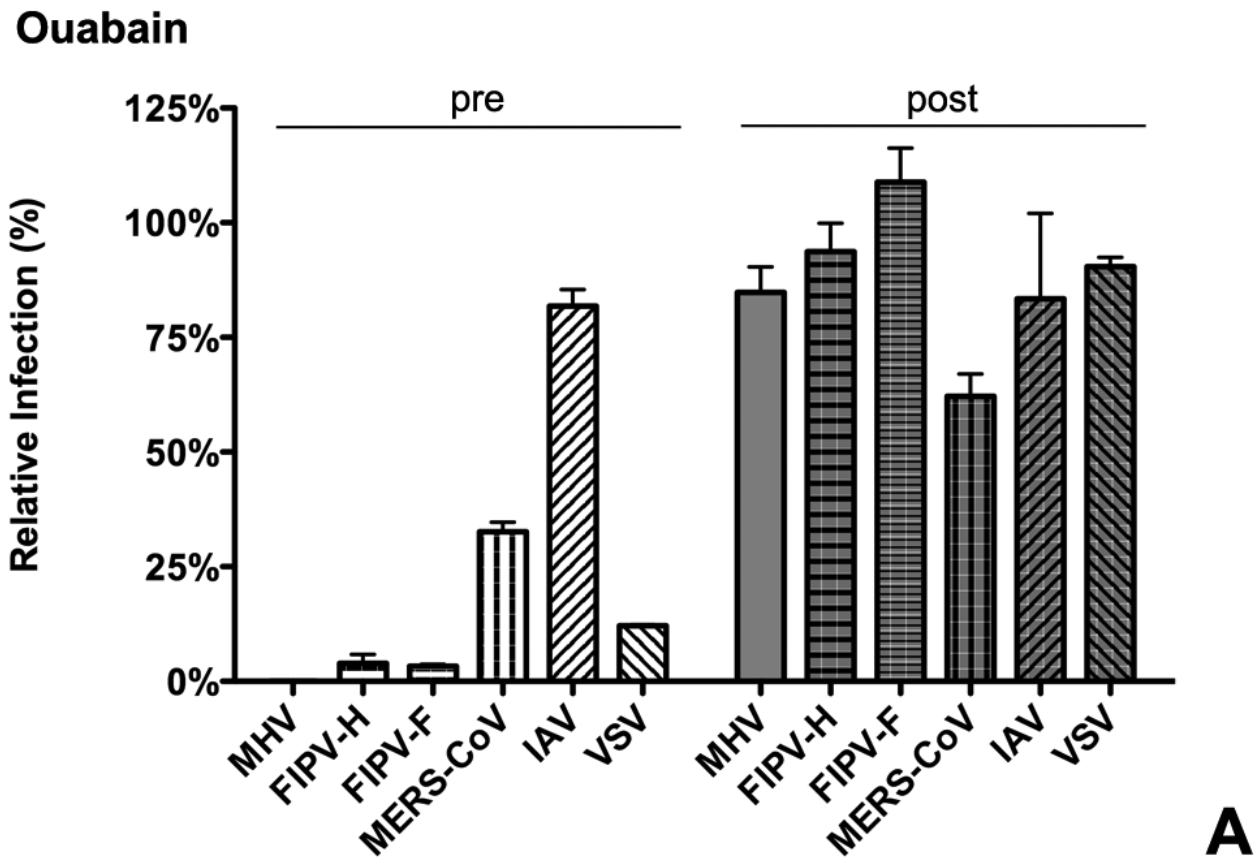

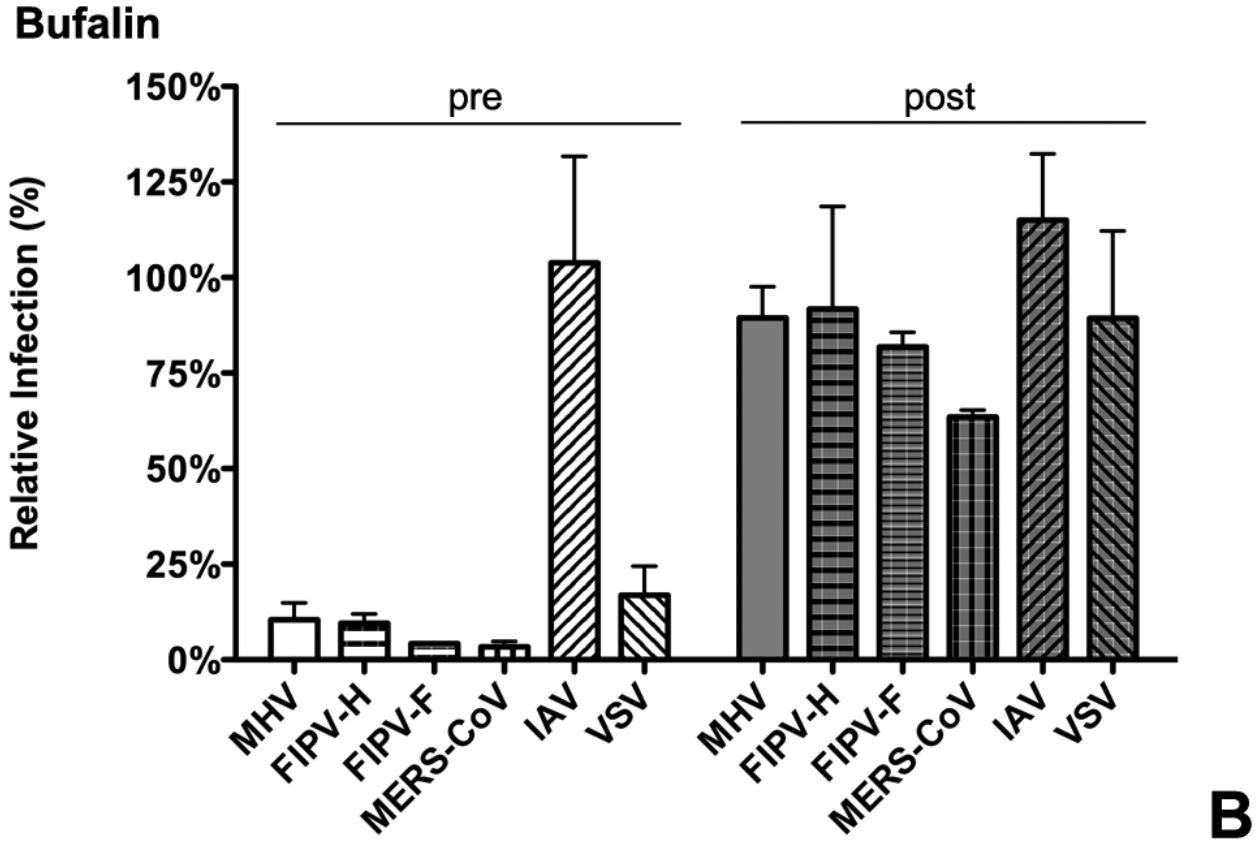

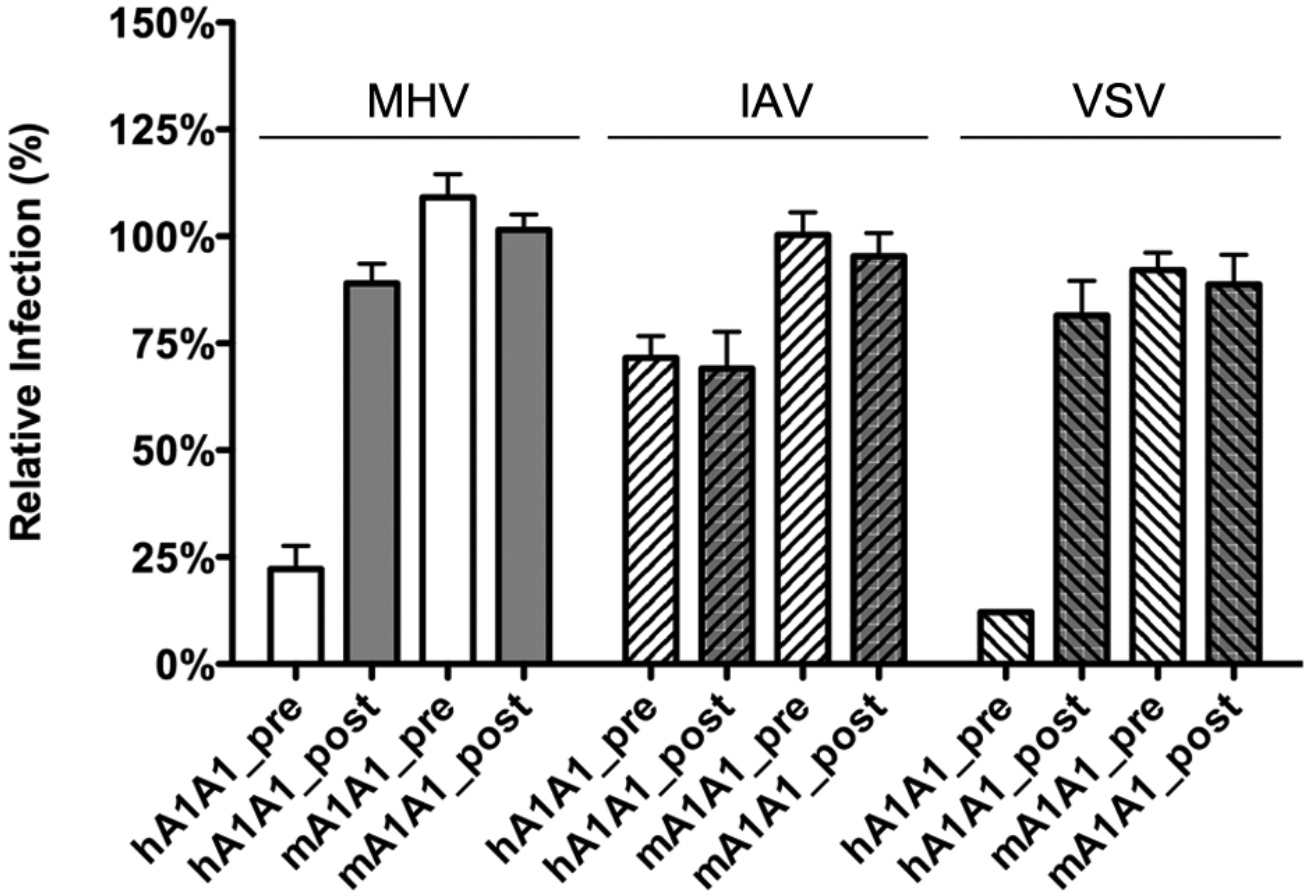

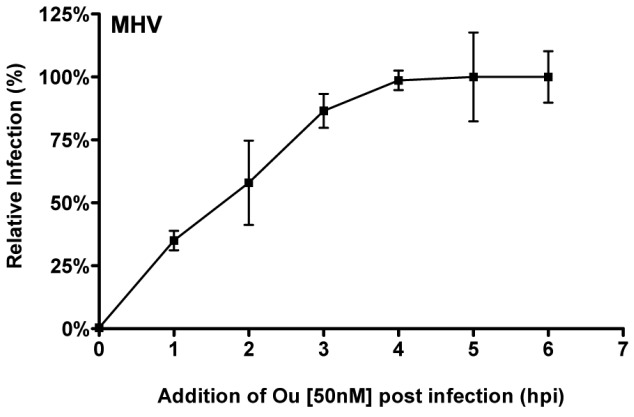

A

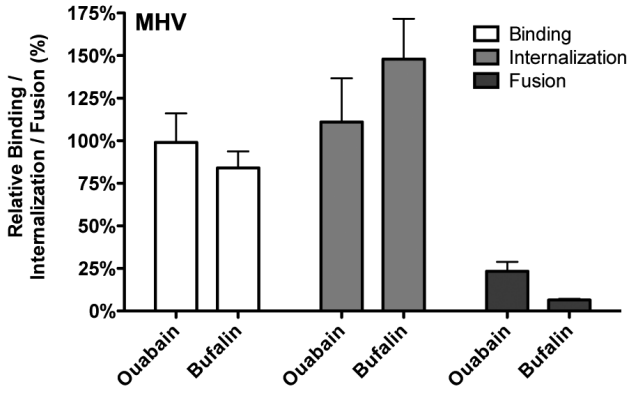

B

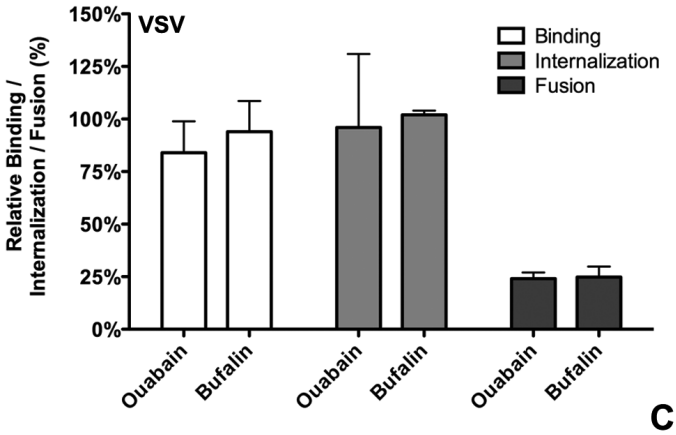

C

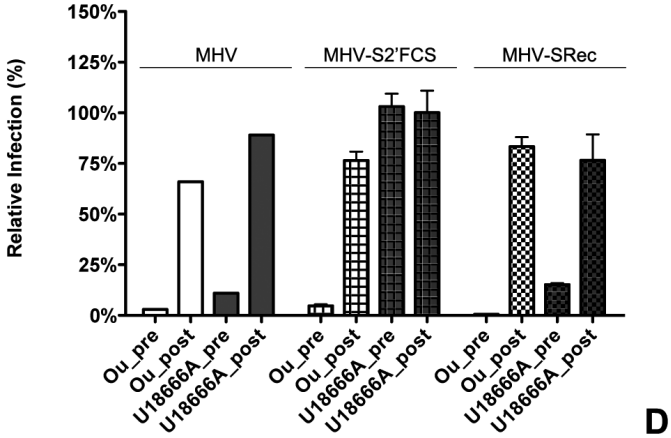

D

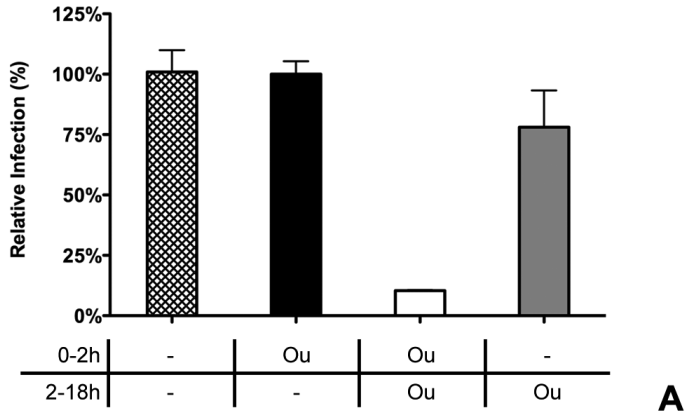

A

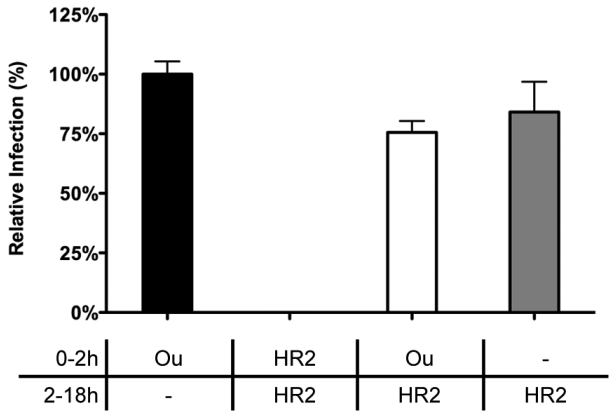

B

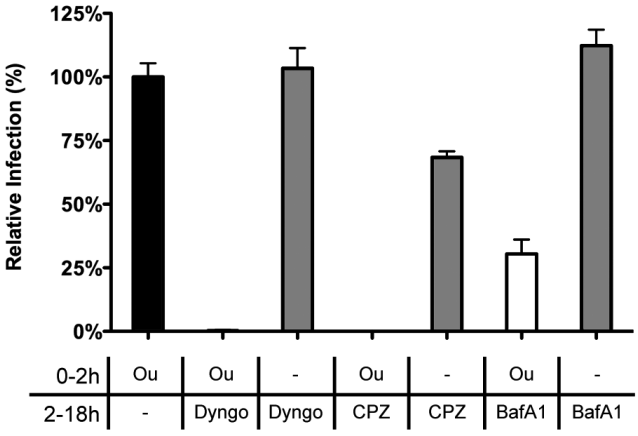

C

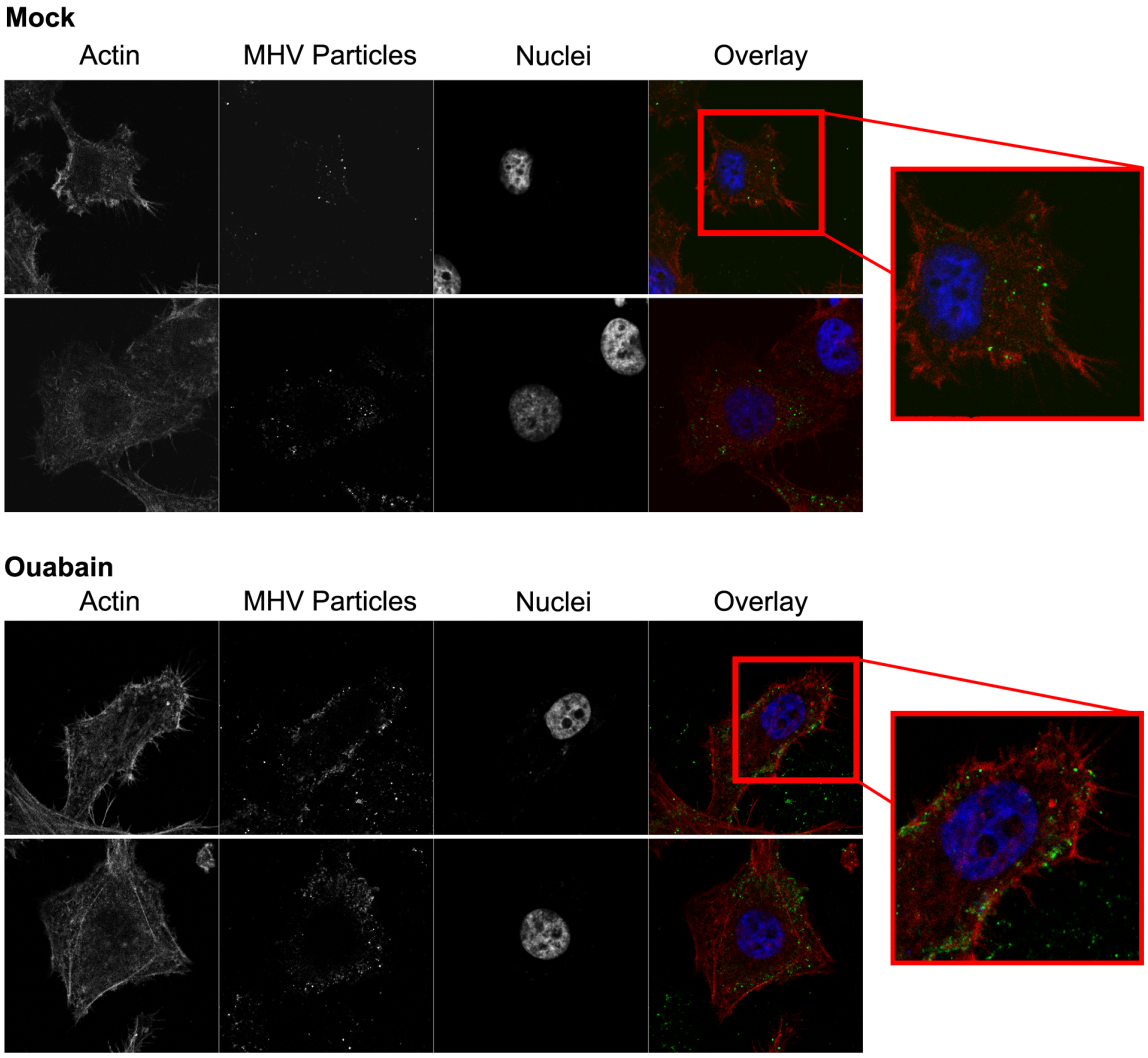

A

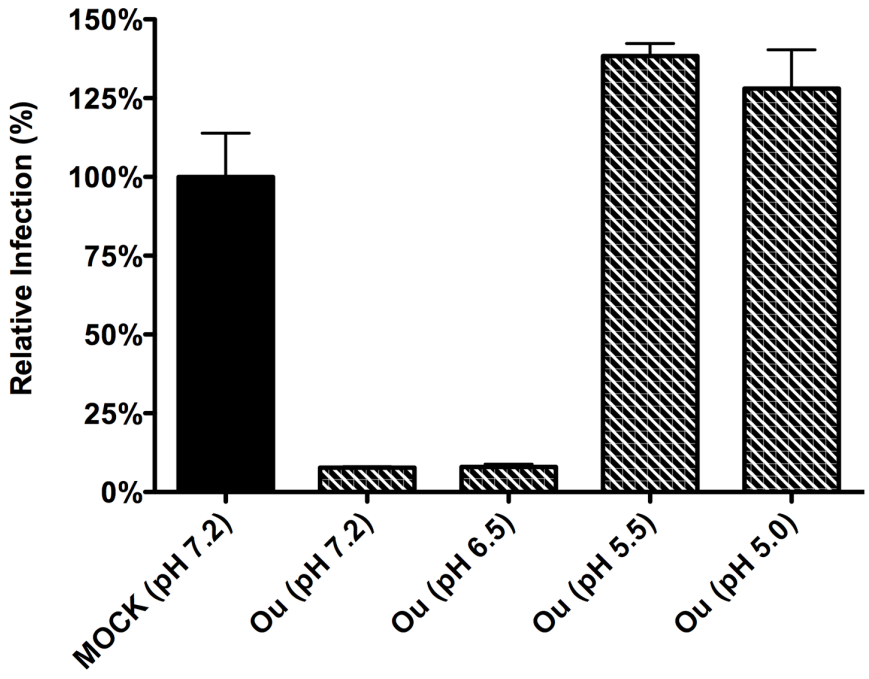

B

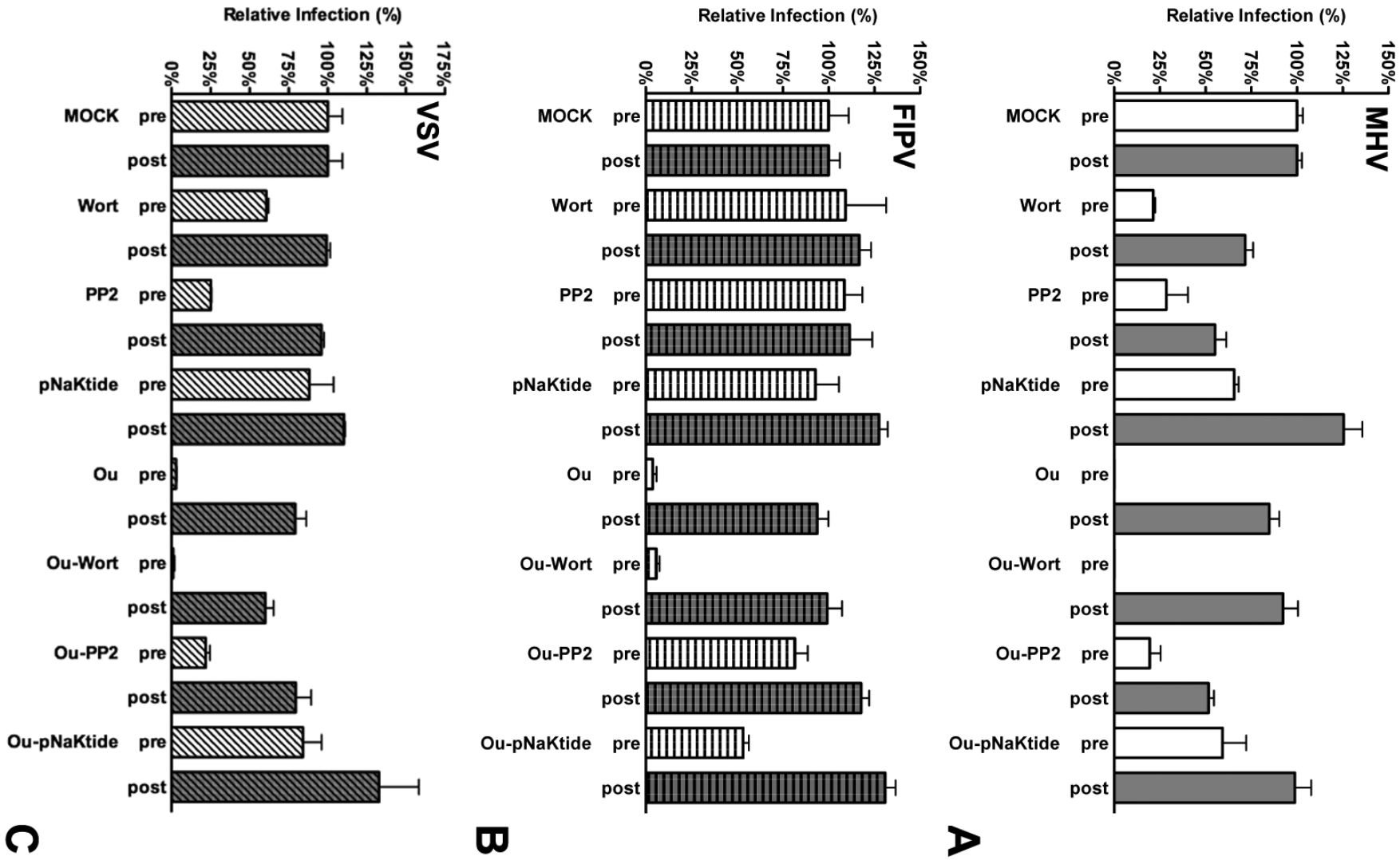
Relative Infection (%)
0%
25%
50%
75%
100%
125%
150%
175%
MHV
FIPV
VSV
MOCK pre
post
Wort pre
post
PP2 pre
post
pNaKtide pre
post
Ou pre
post
Ou-Wort pre
post
Ou-PP2 pre
post
Ou-pNaKtide pre
post
A
B
C